



141  
474  
THS



This is to certify that the  
thesis entitled

NUMERICAL EVALUATION OF PREFERENTIAL FLOW  
THROUGH EVAPOTRANSPIRATIVE LANDFILL COVERS

presented by

Carolyn M. Hardt

has been accepted towards fulfillment  
of the requirements for the

M.S. degree in Civil Engineering

A handwritten signature in black ink, appearing to read "W. L. L. L. L. L.", written over a horizontal line.

Major Professor's Signature

12/5/08

Date

**PLACE IN RETURN BOX** to remove this checkout from your record.  
**TO AVOID FINES** return on or before date due.  
**MAY BE RECALLED** with earlier due date if requested.

| DATE DUE | DATE DUE | DATE DUE |
|----------|----------|----------|
|          |          |          |
|          |          |          |
|          |          |          |
|          |          |          |
|          |          |          |
|          |          |          |
|          |          |          |
|          |          |          |
|          |          |          |
|          |          |          |

**NUMERICAL EVALUATION OF PREFERENTIAL FLOW THROUGH  
EVAPOTRANSPIRATIVE LANDFILL COVERS**

**By**

**Carolyn M. Hardt**

**A THESIS**

**Submitted to  
Michigan State University  
in partial fulfillment of the requirements  
for the degree of**

**MASTER OF SCIENCE**

**Civil Engineering**

**2008**

## **ABSTRACT**

### **NUMERICAL EVALUATION OF PREFERENTIAL FLOW THROUGH EVAPOTRANSPIRATIVE LANDFILL COVERS**

By

Carolyn M. Hardt

Landfill final covers (caps) are regulated by federal and state regulations with the purpose of minimizing the amount of infiltration into the waste (percolation). Conventional cover designs typically consist of a compacted clay layer overlain by a geomembrane. While these covers restrict percolation to relatively small quantities, desiccation cracking of the clay barrier layer is a common long-term shortcoming. Hence, as an alternative, evapotranspirative (ET) covers have been routinely explored. While ET covers can decrease desiccation cracking potential, preferential flow is still a threat. Macropores formed by desiccation, roots, insects, and earthworms are present in almost all soil covers including ET covers.

In this study, preferential flow through an ET cover is evaluated using HYDRUS 1D and 2D (beta version) software which included single-permeability (capillary flow) and dual-permeability (capillary and preferential flow) modeling options. Simulation duration, presence of preferential flow, preferential flow depth, fracture hydraulic conductivity, the amount of fractures, the fraction of surface flow entering the fractures, hydraulic conductivity of the storage layer and waste layer, and waste layer thickness were varied to evaluate their effect on percolation. The key conclusion of this study is that preferential flow can significantly increase percolation through the cap and into the waste layer of a landfill. Ignoring preferential flow, whether it is currently present or will be in the future, can be detrimental when designing and evaluating landfill final covers.

## ACKNOWLEDGMENTS

I would like to thank all individuals who helped me in making this project possible. I wish to express my sincere gratitude to my advisor, Dr. Milind V. Khire, for his guidance and patience. I am also thankful to my committee members, Dr. Mantha and Dr. Wolff, for their valuable time. I also would like to thank Professor Jirka Šimůnek for providing me the beta version of HYDRUS-2D with the dual-permeability modeling option. I would also like to thank Dr. Khire's PhD students Ramil G. Mijares and Moumita Mukherjee for their assistance during the entire process. I acknowledge and am grateful for the financial support extended to me by the Michigan State University for three semesters in the form of a Graduate Teaching Assistantship.

I would like to thank my parents Richard and Margaret and my siblings Tim, Brian and Danielle for their continuing love and encouragement. Apart from them, I would like to thank all my friends and family, especially Robert Aylsworth, Kerry Lewis and Brenda Dill, for their support and encouraging words. Finally, I would like to thank my professors from the Engineering and Geology Departments at the Michigan State University and the Geology Department at the University of Pittsburgh. To everyone I would like to say thank you.

## TABLE OF CONTENTS

|   |            |
|---|------------|
| <b>List of Tables .....</b>   | <b>vi</b>  |
| <b>List of Figures.....</b>   | <b>vii</b> |
| <b>List of Abbreviations .....</b>  | <b>ix</b>  |
| <b>List of Symbols .....</b>  | <b>x</b>   |
| <b>CHAPTER 1: Introduction.....</b>   | <b>1</b>   |
| 1.1 Background.....   | 1          |
| 1.2 Final Covers.....   | 3          |
| 1.2.1 Compacted Clay Barriers.....  | 3          |
| 1.2.2 Evapotranspirative Covers.....  | 3          |
| 1.2.3 Capillary Barrier ET Covers.....                                      | 4          |
| 1.3 Preferential Flow.....  | 8          |
| <b>CHAPTER 2: Estimating Percolation .....</b>                              | <b>9</b>   |
| 2.1 Lysimeters.....   | 9          |
| 2.2 Numerical Modeling.....   | 11         |
| 2.2.1 Uniform Flow.....   | 12         |
| 2.2.2 Non-equilibrium Flow Models .....                                     | 13         |
| 2.2.2.1 Dual-Porosity .....   | 13         |
| 2.2.2.2 Dual-Permeability .....   | 13         |
| <b>CHAPTER 3: HYDRUS.....</b>   | <b>18</b>  |
| 3.1 HYDRUS-2D Overview .....  | 18         |
| 3.1.1 Water Transport .....   | 19         |
| 3.1.2 Dual-Permeability .....   | 20         |
| 3.2 HYDRUS-1D Overview .....  | 21         |
| 3.3 Simulations .....   | 21         |
| 3.3.1 Design .....  | 22         |
| 3.3.2 Soil Hydraulic Properties.....  | 22         |
| 3.3.3 Climate.....  | 26         |
| 3.3.4 Boundary Conditions .....   | 30         |
| 3.3.5 Time Step, Error Tolerance, Mesh Design, and Initial Conditions ..... | 30         |
| 3.3.6 Fracture Properties .....   | 31         |
| 3.3.7 HYDRUS-1D.....  | 31         |
| <b>CHARTER 4: Results and Discussion .....</b>                              | <b>33</b>  |
| 4.1 Presence or Absence of Fractures .....                                  | 35         |
| 4.2 Fracture Properties.....  | 39         |
| 4.2.1 Fracture Depth .....  | 39         |

|  |           |
|--|-----------|
| 4.2.2 Hydraulic Conductivity of Fractures .....                  | 43        |
| 4.2.3 Volume of Fractures .....                                  | 46        |
| 4.2.4 Effect of Fraction of Surface Flow Entering Fractures..... | 48        |
| 4.3 Hydraulic Conductivity of Storage Layer.....                 | 50        |
| 4.4 Waste Layer Parameters .....                                 | 53        |
| 4.4.1 Hydraulic Conductivity of Waste Layer .....                | 55        |
| 4.4.2 Thickness of Waste Layer.....                              | 59        |
| <b>CHAPTER 5: Summary and Conclusions.....</b>                   | <b>62</b> |
| <b>REFERENCES.....</b>   | <b>65</b> |

## **LIST OF TABLES**

|  |           |
|--|-----------|
| <b>Table 3-1: Saturated and Unsaturated Soil Properties .....</b>      | <b>24</b> |
| <b>Table 4-1: Summary of Simulations Carried out Using HYDRUS.....</b> | <b>34</b> |

## LIST OF FIGURES

|   |    |
|---|----|
| Figure 1-1: Cross-Section of a Typical MSW Landfill and Conventional Final Cover (Patel 2005).....  | 2  |
| Figure 1-2: Hydraulic Conductivities of Fine and Coarse Grained Capillary Barrier Soils (Morris and Stormont 1997). ....                        | 6  |
| Figure 1-3: Water-Entry Matric Suction of Two Typical Capillary Barrier Soils (Khire et al. 2000) .....   | 7  |
| Figure 2-1: Cross-Section of a Typical Lysimeter (Albright et al. 2004).....  | 9  |
| Figure 3-1: Schematic of the Conceptual Models used for Numerical Modeling. ....  | 23 |
| Figure 3-2: Soil Water Characteristic Curves. ....  | 25 |
| Figure 3-3: Daily and Cumulative Precipitation Data. ....   | 27 |
| Figure 3-4: Daily and Cumulative PET. ....  | 28 |
| Figure 3-5: Daily Average Temperature and Daily Net Solar Radiation. ....   | 29 |
| Figure 4-1: Simulated Percolation through Cap versus Lysimeter with and without Preferential Flow on a Log Scale (a); and Linear Scale (b)..... | 36 |
| Figure 4-2: Simulated Cumulative Evaporation and Runoff (a); and Simulated Cumulative Percolation through the Bottom Most Boundary (b).....     | 38 |
| Figure 4-3: Depth of Preferential Flow through Lysimeter and Cap.....   | 41 |
| Figure 4-4: Effect of Fracture Depth on Simulated Percolation for Lysimeter (a); and Cap (b). ....  | 42 |
| Figure 4-5: Effect of Waste Layer Hydraulic Conductivity and Fracture Depth on Simulated Percolation. ....                                      | 44 |
| Figure 4-6: Effect of Hydraulic Conductivity of Fractures on Simulated Percolation. ....  | 45 |
| Figure 4-7: Simulated Effect of the Volume of Fractures on Percolation for Lysimeter (a); and Cap (b).....                                      | 47 |
| Figure 4-8: Simulated Effect of $q_{TOP}$ for a Lysimeter (a); and Cap (b). ....  | 49 |

Figure 4-9: Simulated Effect of  $w$  and  $q_{TOP}$  on Percolation through a Lysimeter (a); and Cap (b). ..... 51

Figure 4-10: Effect of Hydraulic Conductivity of the Storage Layer on Simulated Percolation of Lysimeter (a); and Cap (b). ..... 52

Figure 4-11: Simulated Effect of Hydraulic Conductivity of Waste Layer on Cap Percolation without Preferential Flow (a); and with Preferential Flow (b). ..... 54

Figure 4-12: Ratio of Cumulative Percolation with Varying Fracture Depths and Waste Layer Hydraulic Conductivity. .... 58

Figure 4-13: Effect of Waste Layer Thickness on Simulated Percolation..... 61

## **LIST OF ABBREVIATIONS**

**ACAP = Alternative Cover Assessment Project**

**ALCD = Alternative Landfill Cover Demonstration**

**CL = Inorganic clays of low to medium plasticity; gravelly, sandy, silty or lean clays**

**DOE = U.S. Department of Energy**

**ED = Equivalency Demonstration**

**ET = Evapotranspirative/Evapotranspiration**

**HELP = Hydrologic Evaluation of Landfill Performance**

**ML = Inorganic silts and very fine sands, rock flour, silty or clayey fine sands or clayey silts with slight plasticity**

**MSW = Municipal Solid Waste**

**NOAA = National Oceanic and Atmospheric Administration**

**PET = Potential Evapotranspiration**

**RCRA = Resource Conservation and Recovery Act**

**SL = Storage Layer**

**SM = Silty sands, sand-silt mixture**

**SWCC = Soil Water Characteristic Curve**

**USCS = Unified Soil Classification System**

**USEPA = United States Environmental Protection Agency**

**VL = Vegetation Layer**

**WL = Waste Layer**

## LIST OF SYMBOLS

$\alpha$  = van Genuchten Function Fitting Parameter

$\Psi$  = Matric Suction

$\Psi_B$  = Water Entry Matric Suction

$\theta$  = Volumetric Water Content

$\theta_r$  = Residual Water Content

$\theta_s$  = Saturated Water Content

$\gamma_w$  = Dimensionless Scaling Factor

$\Delta S$  = Change in Water Storage

$a$  = Aggregate characteristic length

$\beta$  = Shape Factor

$ET$  = Evapotranspiration

$G$  = Deep Drainage or Percolation into Waste

$h$  = Pressure Head

$K$  = Unsaturated Hydraulic Conductivity

$K_a$  = Interface Hydraulic Conductivity

$K_{ij}^A$  = Components of a Dimensionless Anisotropy Tensor  $K^A$

$K_{FR}$  = Fracture Hydraulic Conductivity

$K_r$  = Relative Hydraulic Conductivity

$K_{sat}$  = Saturated Hydraulic Conductivity

$K_{SL}$  = Storage Layer Hydraulic Conductivity

$K_{VL}$  = Vegetation Layer Hydraulic Conductivity

$K_{WL}$  = Waste Layer Hydraulic Conductivity

$n$  = van Genuchten Function Fitting Parameter

$P$  = Precipitation

$Pr_{CAP}$  = Cumulative Percolation through Cap

$Pr_{LYS}$  = Cumulative Percolation through Lysimeter

$q_{TOP}$  = Amount of Applied Precipitation Entering Directly into the Fractures

$R_i$  = Surface Run-on

$R_o$  = Surface Runoff

$S$  = Sink Term

$t$  = Time

$T_{SL}$  = Storage Layer Thickness

$T_{VL}$  = Vegetation Layer Thickness

$T_{WL}$  = Waste Layer Thickness

$\Gamma_w$  = Transfer Rate

$w$  = Ration of the Volume of the Fracture to the Total System

$x_i$  = Spatial Coordinates

# **CHAPTER 1**

## **INTRODUCTION**

### **1.1 BACKGROUND**

Landfilling is one of the oldest and most common methods of waste disposal used today. In order to assure this system of waste disposal is safe and reliable in the long term, certain measures and regulations must be met. The key components of modern landfills include a bottom liner and leachate collection system (LCS), leachate recirculation system (LRS), gas collection system, surface water management system, and final cover (cap).

The final cover system of a municipal solid waste (MSW) landfill is constructed for the purpose of minimizing exposure of the waste, controlling gas emissions, and preventing the infiltration of water into the waste which could potentially result in the creation of contaminated leachate. Figure 1-1 illustrates a typical MSW landfill and final cover system. Closure criteria for MSW landfills are regulated by Subtitle D, Part 258.60 of the federal Resource Conservation and Recovery Act (RCRA). The final cover must: (1) have a hydraulic conductivity less than or equal to that of any bottom liner system or natural sub-soils present, or a hydraulic conductivity no greater than  $10^{-5}$  cm/s, whichever is less; (2) minimize infiltration through the cover by the use of an infiltration layer that contains a minimum 45 cm of earthen material; and (3) minimize erosion of the final cover by the use of an erosion layer that contains a minimum 15 cm thick soil layer that is capable of sustaining native plant growth. State regulation guidelines may require additional components and restrictions.

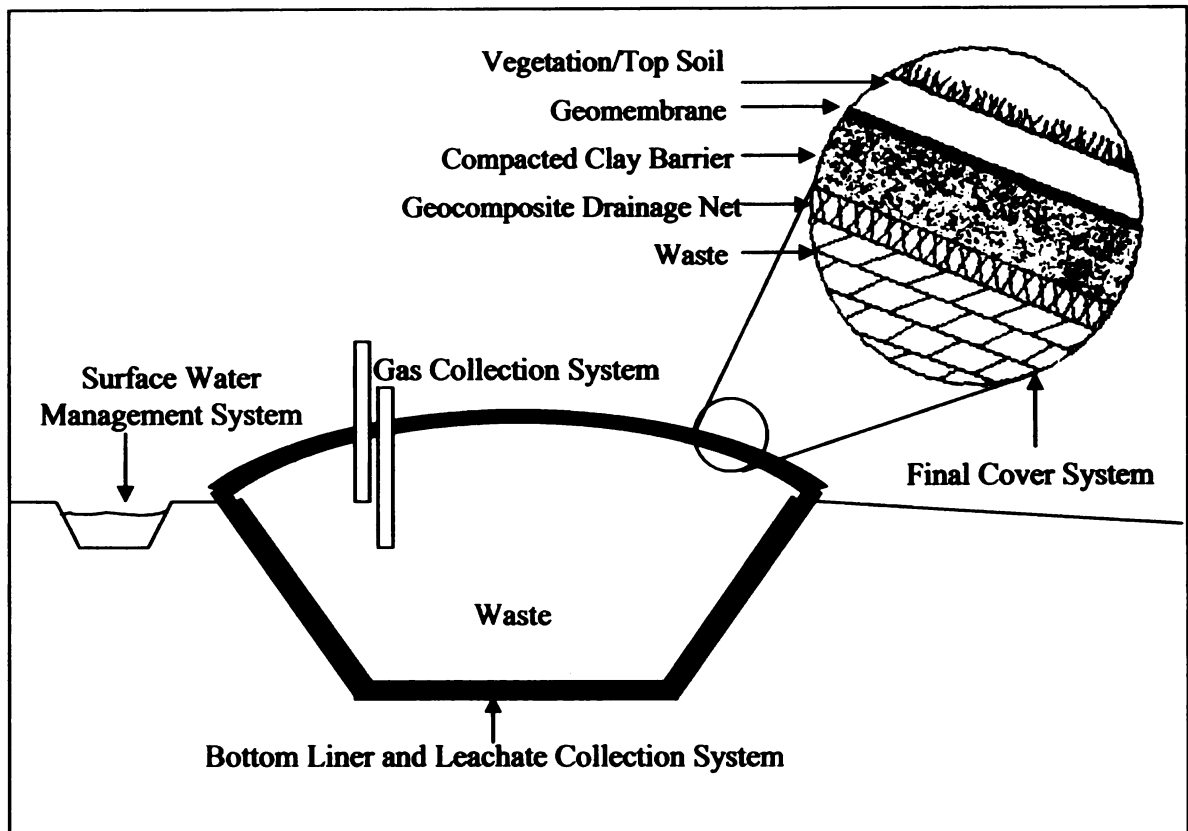


Figure 1-1: Cross-Section of a Typical MSW Landfill and Conventional Final Cover (Patel 2005).

## **1.2 FINAL COVERS**

### **1.2.1 Compacted Clay Barriers**

The resistive, low hydraulic conductivity barrier required by RCRA is intended to minimize water migration into the underlying waste layer. This barrier layer is commonly constructed of compacted clay which often cracks in arid and semi-arid climates due to low precipitation and relatively high evapotranspiration. Clay barriers have been known to crack in sub-humid and humid environments as well (Scanlon et al. 2005). As an alternative to these composite covers consisting of a geomembrane and compacted clay barrier, also known as conventional covers, alternative covers, such as evapotranspirative (ET) covers, have been permitted on a case by case basis.

### **1.2.2 Evapotranspirative Covers**

The RCRA regulations allow for alternative final covers to be implemented as long as their ability to retard infiltration and prevent erosion is equivalent to conventional covers. Instead of relying on “impermeable” barriers, ET covers employ soil water storage capacity and natural evaporation and transpiration to minimize infiltration into the waste layer. These covers are designed to be permeable to precipitation and local run-on which is stored within the soil(s) and later removed by plant transpiration and soil evaporation. A critical component of ET covers is the water storage capacity of the soil. The soil layer(s) must have enough storage capacity to contain all infiltrated water (Khire et al. 1997; 1999). If the storage capacity is exceeded before the water can be removed, water will drain vertically into the underlying waste. In order for ET covers to perform as desired, they must have enough storage capacity to prevent water advancement into the

waste and sufficient evapotranspiration to remove excess water from storage. The governing water balance equation behind ET covers is given in Eq. 1-1:

$$P + R_i = ET + R_o + G + \Delta S \quad (1-1)$$

where  $P$  = precipitation;  $R_i$  = surface run-on from adjacent areas;  $ET$  = evapotranspiration = direct evaporation + transpiration from plants;  $R_o$  = surface runoff;  $G$  = deep drainage or percolation into waste; and  $\Delta S$  = change in the amount of water stored in the cover soils (Jacobson et al. 2005).

Multiple designs of ET covers have been developed over the years including monolithic ET covers, capillary barrier ET covers, and anisotropic barrier ET covers (Benson and Khire 1995). The simplest, monolithic ET covers, consist of only one soil type while more complex designs like the capillary barrier ET cover are comprised of multiply soil types divided into specific layers (Scanlon et al. 2005).

### **1.2.3 Capillary Barrier ET Covers**

Capillary barrier covers consist of a fine-grained soil layer overlying a coarse-grained soil layer which, under unsaturated conditions, acts as a barrier restricting the downward flow of water (Khire et al. 2000). The infiltrating water is held in the fine soil layer until it can be removed by evapotranspirative gradients.

This natural barrier occurs due to the contrast in hydraulic conductivities of the two soils. At high matric potentials, the fine soil will have a small yet finite hydraulic

conductivity while the coarse soil will have a hydraulic conductivity even smaller to the point where it becomes orders of magnitude smaller as seen in Figure 1-2.

While both layers are relatively dry or have a high matric suction, water will not flow downward into the coarse soil but instead will stay in the fine soil, gradually increasing its moisture content which in turn decreases the layer's matric suction and increases its hydraulic conductivity. The decreasing matric suction will eventually reach the effective water-entry suction of the coarse grained soil along the soil interface. The water-entry suction of the coarse soil,  $\Psi_B$ , corresponds to the matric suction located at the bend in the soil water characteristic curve near the residual water content, as shown in Figure 1-3. Once the fine soil reaches  $\Psi_B$ , water begins to enter the coarse soil and the capillary barrier undergoes breakthrough. Just as with the fine soil, the water content and hydraulic conductivity of the coarse soil begins to increase while the matric potential of the layer decreases. Water can now move freely through both cover layers and into the underlying waste layer. The moisture must be removed from the fine grained soil layer before the water-entry matric suction of the coarse soil is reached and the cover is compromised. Removal of moisture can be achieved through evapotranspiration at the surface or lateral drainage along the interface if the surface is sloped or often a combination of the two is used (Morris and Stormont 1997; Khire et al. 2000).

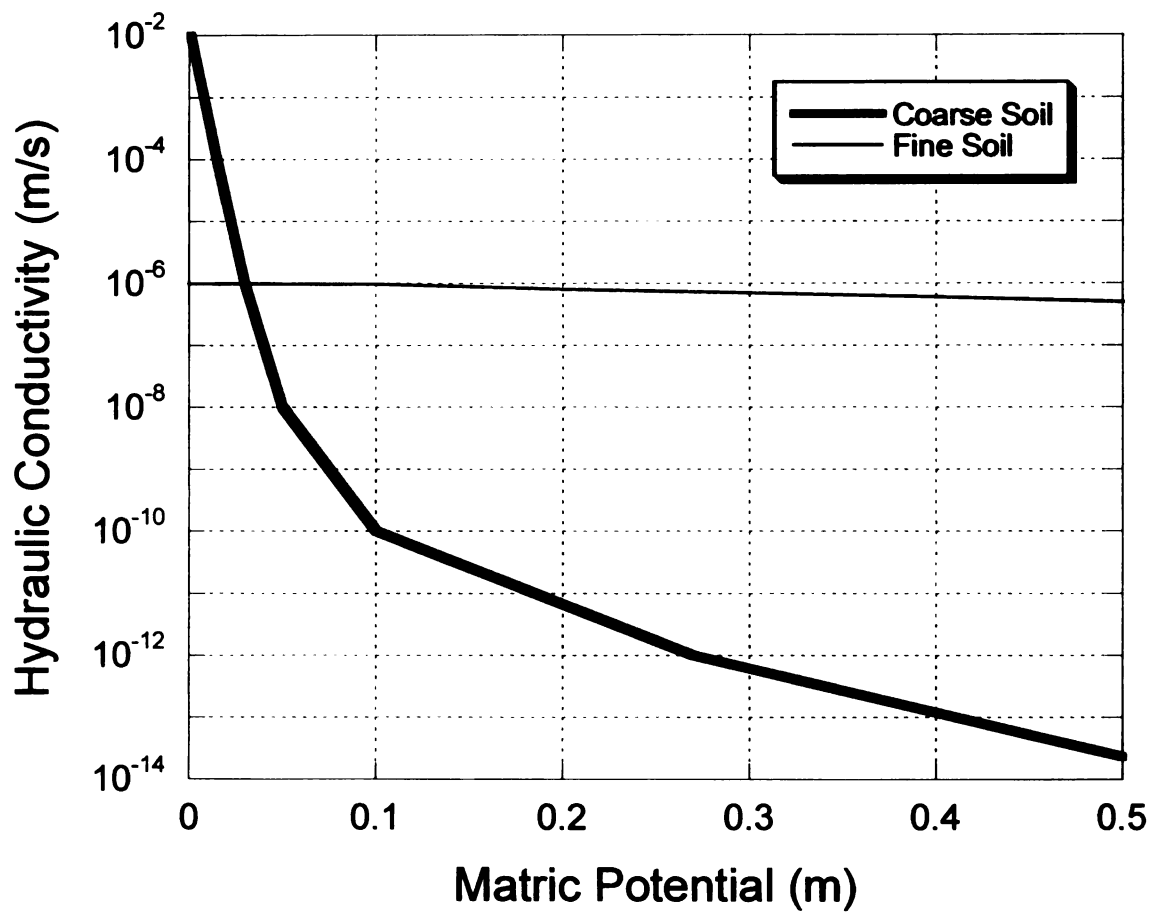


Figure 1-2: Hydraulic Conductivities of Fine and Coarse Grained Capillary Barrier Soils (Morris and Stormont 1997).

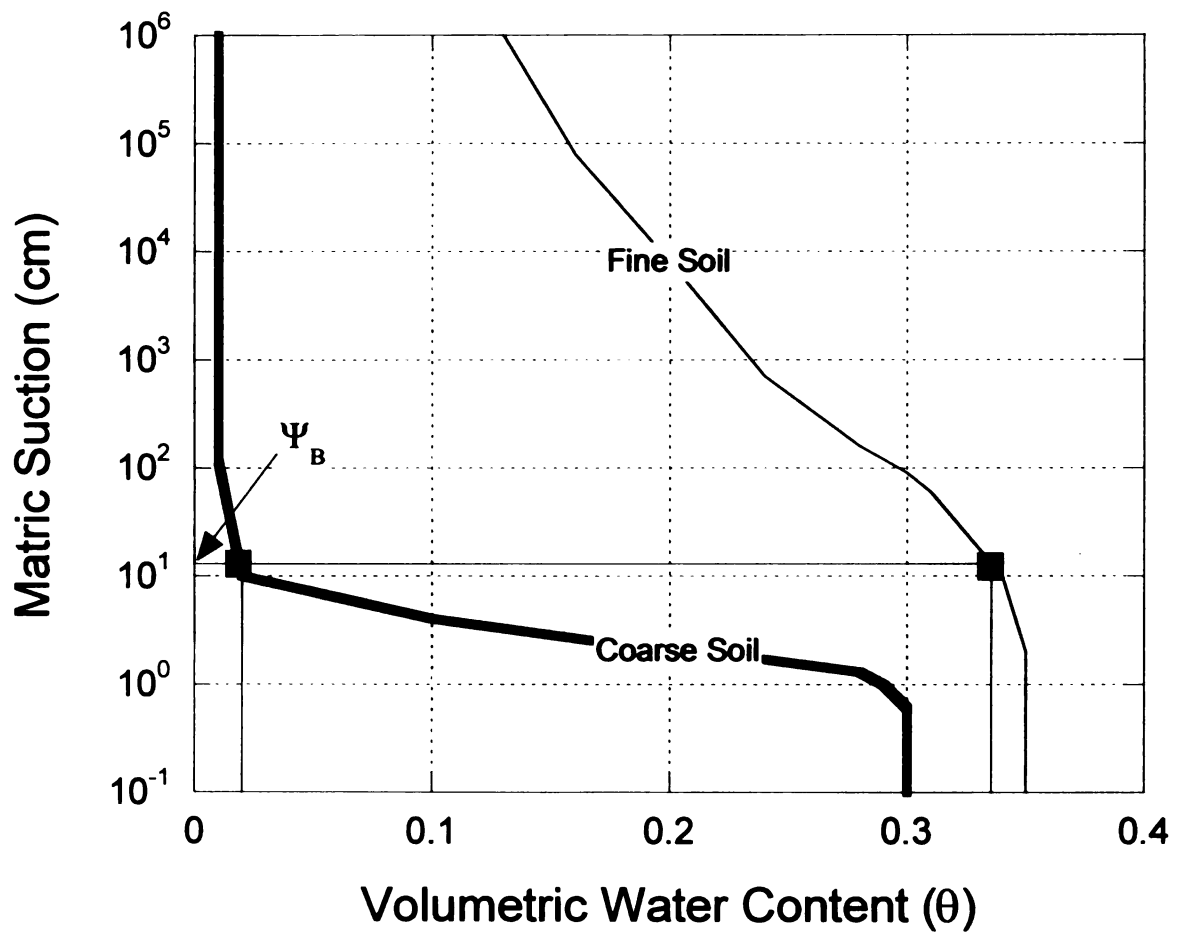


Figure 1-3: Water-Entry Matric Suction of Two Typical Capillary Barrier Soils (Khire et al. 2000).

### **1.3 PREFERENTIAL FLOW**

One of the main failures of conventional final covers is desiccation cracking in the compacted clay layer allowing water to infiltrate into the underlying waste creating potentially harmful leachate. For this reason, much attention has been placed on natural covers such as ET covers. Although ET covers are designed to decrease the chances of desiccation cracking by employing native soils that contain no plastic fines, often it is not possible to eliminate plastic fines. Also, large non-capillary pores (macropores) exist. These macropores are mainly created by desiccation and biological activities due to root channels, insects, and earthworms (Cameira et al. 2000).

Macropores have much higher hydraulic conductivities than the surrounding micropores (referred to as matrix onwards) because they have relatively low water-entry suctions and are often connected to the surface. This allows water to enter easily especially during long or high intensity precipitation events. Depending on their depth, they can transport a significant amount of water at rates orders of magnitude higher than in the matrix. Ignoring infiltration through macropores can lead to an underestimation of percolation, an overestimation of water ponding at the soil surface and high runoff predictions and, as a result, an inadequate prediction of the covers performance (Khire et al. 2000; Novak et al. 2000; Khire and Mijares 2008). In this thesis, all nonuniform infiltration, whether it be cracks, fractures or macropores, is referred to as preferential flow or fracture flow.

## CHAPTER 2

### ESTIMATING PERCOLATION

Before any alternative cover can be used in place of a RCRA cover its ability to minimize infiltration of water into the underlying waste, known as percolation, must be proven to be up to RCRA standards using an approach called the equivalency demonstration (ED). An ED consists of the use of lysimeters and/or instrumented test sections without lysimeters. Sometimes simple analytical or numerical models are also used for the quantitative assessment.

#### 2.1 LYSIMETERS

The use of instrumented lysimeters is the most common method of evaluating the water balance of alternative landfill covers including assessing the amount of percolation. A lysimeter is an impermeable barrier, usually in the shape of a pan, placed under a section of a landfill cover built onsite. A lysimeter usually consists of a drainage layer placed above a geomembrane to collect and measure percolation through the cover (Khire and Mijares 2007). Figure 2-1 shows a schematic of a typical lysimeter.

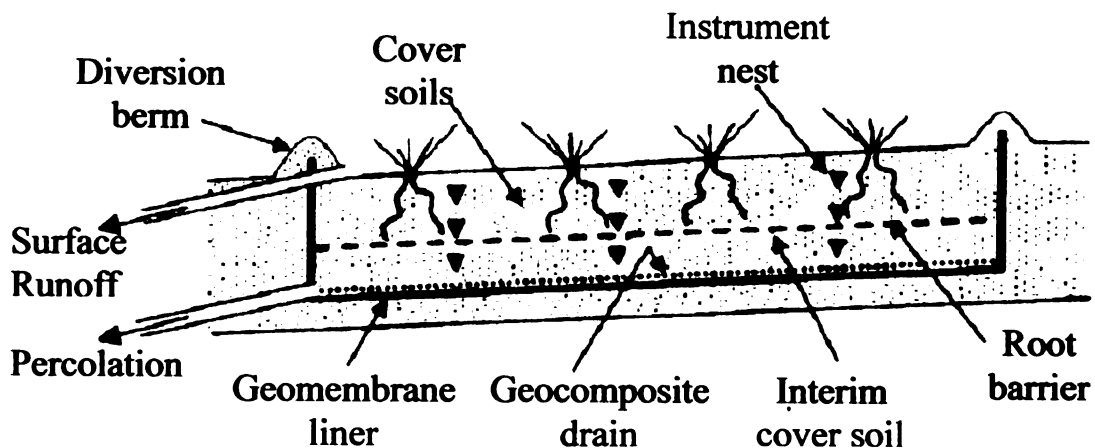


Figure 2-1: Cross-Section of a Typical Lysimeter (Albright et al. 2004).

Between July 1995 and July 2000, the U.S. Department of Energy (DOE) conducted the Alternative Landfill Cover Demonstration (ALCD) in Albuquerque, New Mexico. Six types of covers were built in the field, each 13 m wide and 100 m long, for side by side comparison of performance. Among these, six covers were RCRA Subtitle D and one was a capillary barrier cover. After three years of continuous monitoring, the RCRA covers had an average percolation of 4.82 mm/yr, a 99.98% efficiency rate, and a total percolation of 6,724 L. The efficiency rate is defined as:

$$1 - (\text{percolation} / \text{precipitation}) \times 100 \quad (2-1)$$

The capillary barrier cover had an average percolation of 0.87 mm/yr, an efficiency rate of 99.99%, and a total percolation of 804 L. This ongoing demonstration has shown that not only does the capillary barrier cover prevent percolation as well as a RCRA cover but also can have lower percolation compared to RCRA covers (DOE 2000).

In 1998, the United States Environmental Protection Agency (USEPA) began a similar project, the Alternative Cover Assessment Project (ACAP), where ten conventional cover lysimeters and 14 alternative cover lysimeters were built at 11 different sites in seven states. The primary goal was to measure percolation. Climatic conditions ranged from arid to humid and native soil and native vegetation were used at all sites. Percolation was monitored from July 1 to June 30 of the following year beginning in 2000 and ending in 2003. At the sub-humid site in Polson, MT, a capillary barrier cover and a conventional cover were constructed. The conventional cover had a total percolation of 15 mm during the designated monitored time and an average of 0.4

mm/yr. The capillary barrier performed better having a total percolation of 0.2 mm during the three year period (Albright et al. 2004). As with the DOE study, the capillary barrier cover proved to be more than equivalent to a RCRA Subtitle D cover during the three year monitoring period.

With the use of lysimeters, it has been demonstrated that capillary barrier evapotranspirative covers can be considered equivalent to the RCRA Subtitle D cover. Not only do they prevent a significant amount of percolation from passing through the cover but also reduce percolation, exceeding the RCRA standards.

## **2.2 NUMERICAL MODELING**

Relying solely on the use of lysimeters for an estimation of percolation can be misleading. Khire and Mijares (2008) demonstrated using the water balance model Vadose/W (by Geo-Slope 2007) that the presence of an underlying waste layer in an actual cover influences percolation. Because lysimeters have a geomembrane underneath the proposed cover system instead of a waste layer, as soon as percolation passes through the cover it is removed from the system. In an actual cover, a waste layer is present which can hold water and allow it to migrate upwards back into the cover due to evapotranspirative gradients. All simulations in the study (Khire and Mijares 2008) resulted in the over-estimation of percolation by the lysimeter compared to percolation amounts of a cover and waste layer system for a simulated site located in Detroit, Michigan. In this study only capillary flow was considered. Flow through macropores was not simulated because Vadose/W (Geo-Slope 2007) does not have an option to simulate preferential flow. Khire and Mijares (2008) have proposed a numerical approach to estimate percolation from a cover and waste layer system.

### **2.2.1 Uniform Flow**

Uniform, equilibrium, or single-porosity/single-permeability models are based on the concept that water and/or solutes enter and penetrate through a soil profile in a uniform manner. This type of flow can naturally occur in granular soils but is often incorrectly applied when modeling finer soils and soils containing plant roots and insect or animal burrows. Most uniform flow models apply Richards equation to the entire porous media as a whole. These models are easier to use because they only require one set of soil hydraulic properties but can produce misleading results when preferential flow is significant (Gärdenäs et al. 2006). HELP (Hydrologic Evaluation of Landfill Performance), UNSAT-H, LEACHM, Vadose/W and HYDRUS v2.007 are some of the most popular uniform flow models today (Šimůnek et al. 2003; Kodešová et al. 2005; Ogorzalek et al. 2008).

Numerical modeling with uniform models can be a helpful tool when assessing a landfill's performance but should be used with caution. HELP is often used by geotechnicians to predict percolation through landfill covers. However, Khire et al. (1997) found that HELP significantly over-predicts percolation. In the same study, UNSAT-H was also analyzed and was found to slightly under-predict percolation compared to measured field data. Benson et al. (2005) re-confirmed these findings with data from the ACAP study. Yet in another study by Khire et al. (1999), UNSAT-H over-predicted percolation. In other studies, Vadose/W was shown to under-predict percolation (Benson et al. 2005) and HYDRUS v2.007, LEACHM v4.0 and UNSAT-H v.3.0 all over-predicted percolation (Ogorzalek et al. 2008).

Uniform flow numerical models can be a useful tool when it comes to predicting landfill cover percolation but the accuracy will depend on how significant the macropore

flow component is for the problem. A margin of error always exists and should be taken into consideration. Some inaccuracy may be due to the varying levels of complexity and sophistication between the models. Other models such as HELP have known limitations due to the simplistic water routing approach used (Morris et al. 1997 and Khire et al. 1997). One of the flaws uniform models share is not accounting for preferential flow which can lead to an underestimation of percolation. This common blemish in numerical modeling is significant and hence has been the focus of this thesis.

### **2.2.2 Non-equilibrium Flow Models**

Non-equilibrium flow was defined by Jarvis (1998) as any system where “for various reasons, infiltrating water does not have sufficient time to equilibrate with slowly moving resident water in the bulk of the soil matrix.” Non-equilibrium or preferential flow is simply the phenomenon of infiltrating water entering a fracture or macropore of some sort in the soil causing the water in the fracture to penetrate the soil faster than the water in the surrounding soil matrix. In order to achieve more accurate predictions when modeling water balance in soils and landfill covers, it is critical to account for preferential flow. The difficulty in modeling cracks, fractures and macropores lies in the accuracy of estimating parameters that can accurately characterize the preferential flow paths and numerical algorithms that are able to carry out the necessary computations in a reasonable time frame with an acceptable level of accuracy. Not only does preferential flow affect the estimation of percolation through landfill covers but can also affect solute transport modeling and irrigation efficiency modeling for agricultural and other applications (Novák et al. 2000; Šimůnek et al. 2003).

#### 2.2.2.1 Dual-Porosity

Dual-porosity models separate the soil matrix and fractures into two different water regimes. Water flow in the soil matrix is stagnant allowing water to only flow in the fracture network (Šimůnek et al. 2003). The soil matrix can retain, store and exchange water but does not allow for continuous flow. Many dual-porosity models apply Richards equation to the water flow in the fractures and a mass balance equation to the soil matrix. Alternatively, a kinematic wave equation describing gravitational water flow can also be applied to the fractures. This approach eliminates the need for soil hydraulic properties of the fracture system, which can be difficult to determine, but can not be applied to two-dimensional flow (Šimůnek et al. 2003).

#### 2.2.2.2 Dual-Permeability

Dual-permeability models are similar to dual-porosity models except water can flow in the soil matrix as well as in the fractures. Although this addition can lead to more realistic results, more input parameters such as those relating to the matrix, fracture and matrix-fracture interface are required that often cannot be directly measured, increasing the possibility of error (Šimůnek et al. 2003). Dual-permeability models are becoming more common for modeling preferential flow in soils. The benefits of using dual-permeability versus single-permeability are amplified not only in modeling preferential flow in landfill covers but also in irrigation and soil contamination. Much of the evaluation of dual-permeability models has been in the agricultural industry (Šimůnek et al. 2003; Kodešová et al. 2005).

Soil contaminated by the use of pesticides is a major environmental concern in agriculture. Although contaminant concentrations in the soil can be monitored, it is an

expensive and time consuming process which has led to the use of numerical models to simulate the distribution of pesticide in the soil profile as an alternative. However, the distribution of contaminants in the soil often varies between what is observed and what is simulated due to preferential flow. Kodešová et al. (2005) used HYDRUS-1D to simulate the distribution of chlorotoluron in the soil profile using both single-porosity and dual-permeability methods and compared the results to measured field data. The single-porosity model predicted that chlorotoluron reaches to a depth of 8 cm while the dual-permeability predicted that it reaches to a depth of 60 cm which was much closer to the observed behavior of the chlorotoluron. It was concluded that the dual-permeability model performed significantly better and more closely matched observed data than the single-porosity model.

Gerke and Köhne (2004) conducted a bromide tracer experiment to analyze if DUAL, a relatively simple dual-permeability model, could accurately model the preferential flow of bromide. Simulations were also carried out using HYDRUS with the single-permeability model for comparison. 16.75 kg of potassium bromide was applied to a tile-drained glacial till field near the Northern Germany city of Kiel. After 138 days, the measured cumulative outflow amounted to 27.7 cm and DUAL predicted an outflow of 28.6 cm but over predicted outflow in the beginning and under predicted it towards the end. HYDRUS had similar results. However, when it came to predicting bromide concentrations DUAL was able to closely simulate observed temporal patterns while HYDRUS failed to estimate any bromide concentrations.

Gärdenäs et al. (2006) compared the ability of four preferential flow modeling approaches to simulate drainage and pesticide leaching into a tile-drained agricultural

field. The four models, carried out in HYDRUS-2D, include: (1) an equilibrium approach model; (2) a non-equilibrium mobile-immobile transport model combined with standard equilibrium flow; (3) a non-equilibrium dual-porosity approach model; and (4) a non-equilibrium dual-permeability model. The numerical models were compared to field data from a site in Näsbygård, Sweden. The site has a warm-temperate climate and an average annual precipitation rate of 662 mm. The non-equilibrium mobile-immobile model produced the same water balance as the equilibrium model. The equilibrium model captured the correct cumulative drainage for a peak period in June but only estimated one-third of the flow of the largest peak flow measured. The equilibrium flow model also simulated the peak flows days later than when they actually occurred. The dual-porosity and dual-permeability models both captured the timing of the first peak correctly but overestimated the amount of drainage. The dual-porosity model overestimated the drainage by a factor of 2.5 and the dual-permeability model overestimated the drainage by a factor of 5.6. The models produced similar results when it came to simulating pesticide concentrations. In the end, the dual-permeability model simulated the dynamics of the pesticide most accurately but overestimated the total drainage.

Now that dual-permeability models are emerging as the more favorable way to model preferential flow, their application to modeling percolation through landfill covers must be analyzed because preferential flow has been reported in many studies. It is critical to understand how preferential flow can affect percolation into the waste layer especially when proposing the use of an alternative landfill cover. The purpose of this thesis is to numerically evaluate preferential flow through ET covers using the dual-permeability

model of HYDRUS-2D and HYDRUS-1D and how percolation is affected by specific aspects of cover design.

## **CHAPTER 3**

### **HYDRUS**

HYDRUS-2D (beta v1.04) and HYDRUS-1D (v4.05) were used to evaluate preferential flow in ET landfill covers in this study. Simulations modeled these two ET cover systems: (1) a vegetative soil layer underlain by a storage layer with a lysimeter boundary (without waste layer), and (2) a vegetative soil layer underlain by a storage layer which is underlain by a waste layer (simulating a cap). HYDRUS was selected for multiple reasons: (1) HYDRUS is a water balance model which has been used to simulate the water balance of earthen caps (Sadek et al. 2007); (2) HYDRUS also has a dual-permeability option which was confirmed by Šimůnek et al. (2003) and Gärdenäs et al. (2006); and (3) it is the only commercially available water balance model for which currently a dual-permeability option is available to simulate preferential flow. The key purpose of these simulations was to quantify the effect of preferential flow on percolation for lysimeters versus for actual ET caps. The following chapter describes the numerical model HYDRUS and how it was used in this study. The simulations results are discussed in Chapter 4.

#### **3.1 HYDRUS-2D OVERVIEW**

HYDRUS-2D (beta v1.04) was used for the majority of simulations. This finite element program is designed to model water, heat, and solute transport in a two-dimensional variably saturated media. For the purpose of this study, only water transport was simulated.

### 3.1.1 Water Transport

Water flow in HYDRUS-2D is governed by a modified form of Richards equation:

$$\frac{\partial \theta}{\partial t} = \frac{\partial}{\partial x_i} \left[ K \left( K_{ij}^A \frac{\partial h}{\partial x_j} + K_{iz}^A \right) \right] - S \quad (3-1)$$

where  $\theta$  = volumetric water content [ $L^3 L^{-3}$ ];  $h$  = the pressure head [L];  $S$  = sink term [ $T^{-1}$ ];  $x_i$  ( $i=1,2$ ) = spatial coordinates [L];  $t$  = time [T];  $K_{ij}^A$  = components of a dimensionless anisotropy tensor  $K^A$ ; and  $K$  = unsaturated hydraulic conductivity [ $LT^{-1}$ ] given by:

$$K(h, x, z) = K_{sat}(x, z) K_r(h, x, z) \quad (3-2)$$

where  $K_r$  = relative hydraulic conductivity; and  $K_{sat}$  = saturated hydraulic conductivity [ $LT^{-1}$ ]. These equations were designed for a two-dimensional, isothermal Darcian flow of water in a variably saturated porous medium. It assumes the air phase is insignificant when considering water flow.

The user can select between multiple analytical models for describing the unsaturated hydraulic properties of the soils such as van Genuchten-Mualem, Modified van Genuchten, and Brooks-Corey models. All simulations in this study used a dual-permeability model not available to the public in the 2D version. The option of hysteresis is also available but was not used (Šimůnek et al. 1999).

### 3.1.2 Dual-Permeability

To simulate dual-permeability, the model assigns two soil properties to the porous media, one pertaining to the fracture network (macropores) and one to the soil matrix (micropores). The soil matrix and fracture network are modeled as a continuum. Richards equation is applied to both the matrix region and the fracture (preferential flow) region. This modified Richards equation solves for the changes in volumetric water content in the soil matrix with time by combining the flow of water due to advective and dispersion (for solute transport) forces with the water transferred from the fracture domain. A sink term is also added to account for any water loss from the matrix. The water flow equation for the matrix (subscript m) is:

$$\frac{\partial \theta_m}{\partial t} = \frac{\partial}{\partial z} \left( K_m \frac{\partial h_m}{\partial z} + K_m \right) - S_m + \frac{\Gamma_w}{1-w} \quad (3-3)$$

and the equation for flow within the fractures (subscript f) is:

$$\frac{\partial \theta_f}{\partial t} = \frac{\partial}{\partial z} \left( K_f \frac{\partial h_f}{\partial z} + K_f \right) - S_f + \frac{\Gamma_w}{w} \quad (3-4)$$

where  $w$  = the ratio of the volume of the fracture domain to the total volume of the system; and  $\Gamma_w$  = the transfer rate of water from the fracture to the matrix and is calculated as follows:

$$\Gamma_w = \frac{\beta}{a^2} K_a \gamma_w (h_f - h_m) \quad (3-5)$$

where  $\beta$  = the aggregate shape factor;  $a$  = the aggregate characteristic length;  $K_a$  = interface hydraulic conductivity; and  $\gamma_w$  = the dimensionless scaling factor. The dual-permeability model is computationally much more complicated than the general flow equation (Eq. 3-1) because now the characterization of hydraulic conductivity functions and water retention are computed for both regions along with the hydraulic conductivity function for the matrix-fracture interface (Šimůnek et al. 2003; Kodešová et al. 2005; and Vogel et al. 2000).

### 3.2 HYDRUS-1D OVERVIEW

HYDRUS-1D was released in February of 2008 with a publicly accessible dual-permeability option. This model was released after the majority of simulations in this study were carried out using the HYDRUS-2D beta version. Hence, only a small number of simulations were carried out using the 1D model, primarily to “confirm” the results of the 2D beta version. The 1D version of HYDRUS is similar to HYDRUS-2D previously discussed except that it simulates only one-dimensional water flow.

### 3.3 SIMULATIONS

Specific properties and input parameters required for HYDRUS-2D and HYDRUS-1D are discussed below. Unless otherwise stated, these properties remained constant throughout all simulations.

### **3.3.1 Design**

2D representations of ET covers with preferential flow were created using HYDRUS-2D software to evaluate percolation when specific parameters were varied. The climatic data collected from a landfill site in Detroit, Michigan was used for all simulations. This site is located in a sub-humid region. The covers consisted of a 0.3 m thick vegetation layer (VL) above a 1 m thick storage layer (SL). In simulations that simulated an actual cap system, a 6.1 m thick waste layer (WL) was added underneath the cover. However, some simulations purposely excluded this waste layer in order to simulate a lysimeter and in four simulations the waste layer thickness was decreased to 3.05 m or increased to 12.2 m to evaluate the sensitivity of this parameter. The width and horizontal depth of the models were fixed at 1 m. Mesh lines were placed across all horizontal boundaries and in between all layers to output water flux across the boundary. A schematic of the conceptual models is presented in Figure 3-1.

### **3.3.2 Soil Hydraulic Properties**

Various hydraulic conductivities of the storage layer ( $1 \times 10^{-4}$ ,  $1 \times 10^{-5}$ , and  $1 \times 10^{-6}$  cm/s) and waste layer ( $1 \times 10^{-3}$ ,  $1 \times 10^{-4}$ , and  $1 \times 10^{-5}$  cm/s) were input in several simulations, while the hydraulic conductivity of the vegetation layer was maintained at  $1 \times 10^{-3}$  cm/s. The saturated and unsaturated soil properties and fitting parameters used for describing the soil water characteristic curves (SWCC) corresponding to each hydraulic conductivity are listed in Table 3-1. The SWCCs are plotted in Figure 3-2.



Table 3-1: Saturated and Unsaturated Soil Properties

| Layer | Thickness (m) | $K_{sat}$ (cm/s)   | $\theta_r$ (cm <sup>3</sup> /cm <sup>3</sup> ) | $\theta_s$ (cm <sup>3</sup> /cm <sup>3</sup> ) | $\alpha$ (cm <sup>-1</sup> ) | n      | USCS Classification | Source                   |
|-------|---------------|--------------------|--|--|------------------------------|--------|---------------------|--------------------------|
| VL    | 0.3           | $1 \times 10^{-3}$ | 0  | 0.41   | 0.0072                       | 1.3182 | ML-CL               | Khire and Mijares 2008   |
| SL    | 1             | $1 \times 10^{-4}$ | 0.02   | 0.35   | 0.012                        | 1.123  | SM-ML               | Khire et al. 2000 & 2008 |
|       |               | $1 \times 10^{-5}$ | 0  | 0.41   | 0.0072                       | 1.3182 | ML-CL               | Khire and Mijares 2008   |
|       |               | $1 \times 10^{-6}$ | 0.08   | 0.52   | 0.035                        | 1.25   | ML                  | Khire et al. 2000 & 2008 |
| WL    | 3, 6, or 12   | $1 \times 10^{-3}$ | 0.11   | 0.53   | 0.26                         | 2.22   | MSW                 | Benson and Wang 1998     |
|       |               | $1 \times 10^{-4}$ | 0.02   | 0.35   | 0.012                        | 1.123  | SM-ML               | Khire et al. 2000 & 2008 |
|       |               | $1 \times 10^{-5}$ | 0  | 0.41   | 0.0072                       | 1.3182 | ML-CL               | Khire and Mijares 2008   |

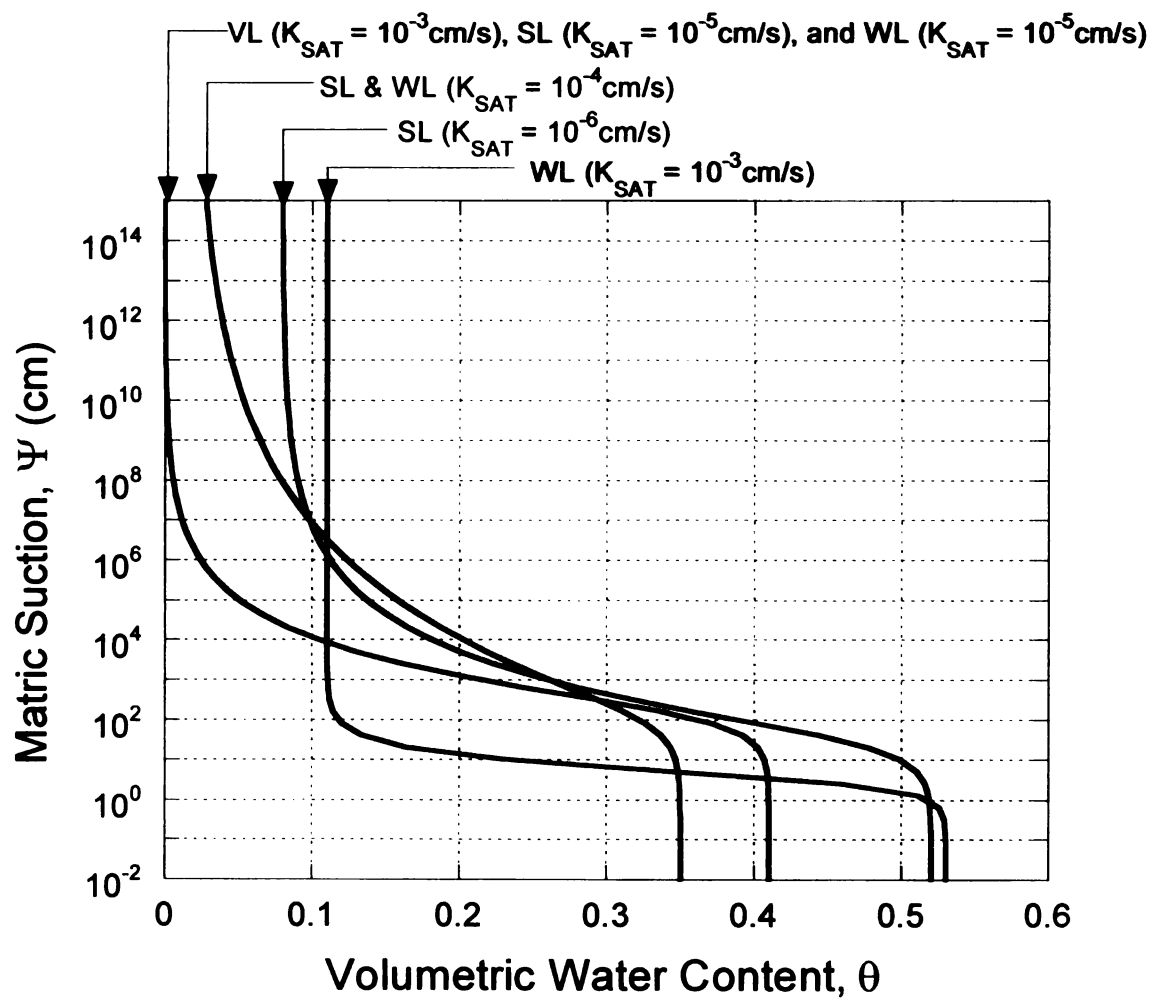


Figure 3-2: Soil Water Characteristic Curves.

### **3.3.3 Climate**

Precipitation and potential evaporation data was derived from measured field data from a landfill site in Detroit, Michigan from January to December 2006. Collection of the meteorological data was completed by Khire and Mijares (2008). Hourly meteorologic data was recorded from February 2005 to December 2006 including the maximum and minimum temperatures, wind speed, and precipitation. Relative humidity data was obtained from a local National Oceanic and Atmospheric Administration (NOAA) weather station. GeoSlope's Vadose/W (2007) was used to estimate the potential evapotranspiration (PET) and net solar radiation based on a latitude of 42.38° from the measured meteorological data. Effects of transpiration were ignored by assuming a bare ground surface to produce conservative PET rates. For the purpose of this study, only data from January 1, 2006 to December 31, 2006 was used. In the case of a two year simulation, the 2006 meteorological data was repeated. The total precipitation for 2006 was 857.5 mm and the total estimated PET was 1021.9 mm. The daily and cumulative distribution of precipitation, PET, and daily temperature and net solar radiation are plotted in Figures 3-3, 3-4 and 3-5, respectively.

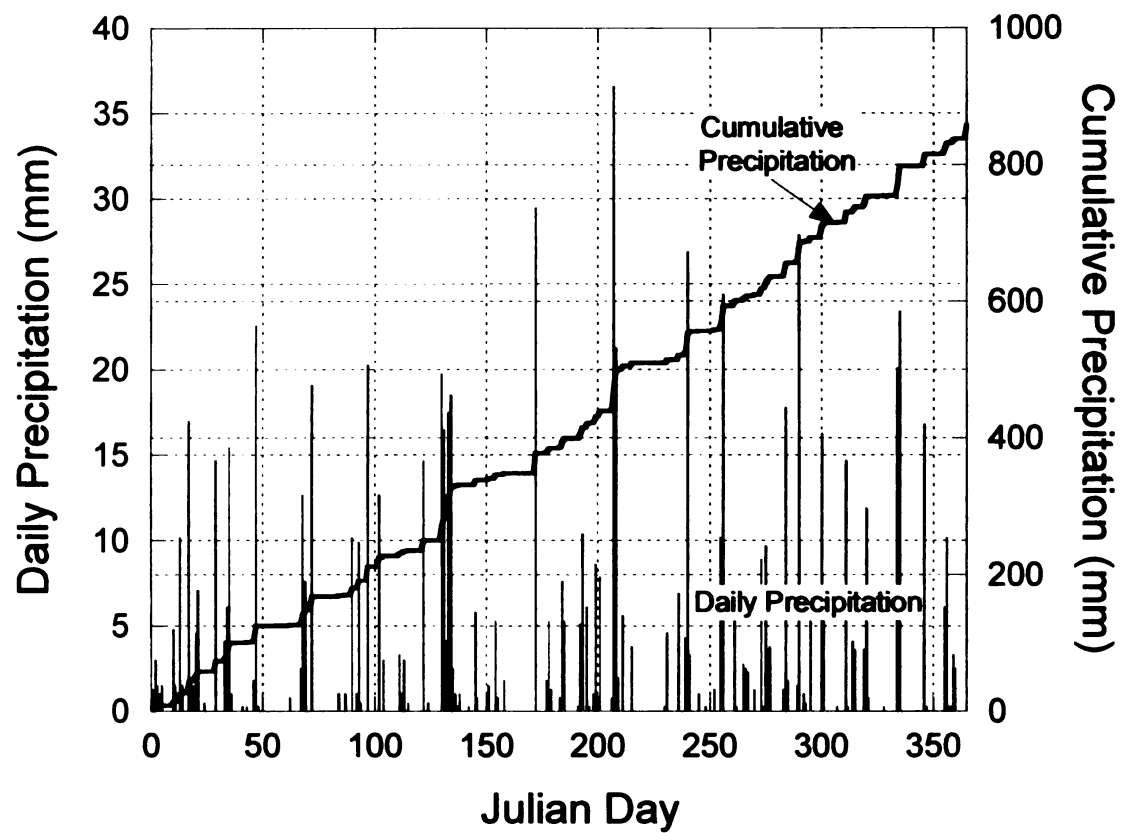


Figure 3-3: Daily and Cumulative Precipitation Data.

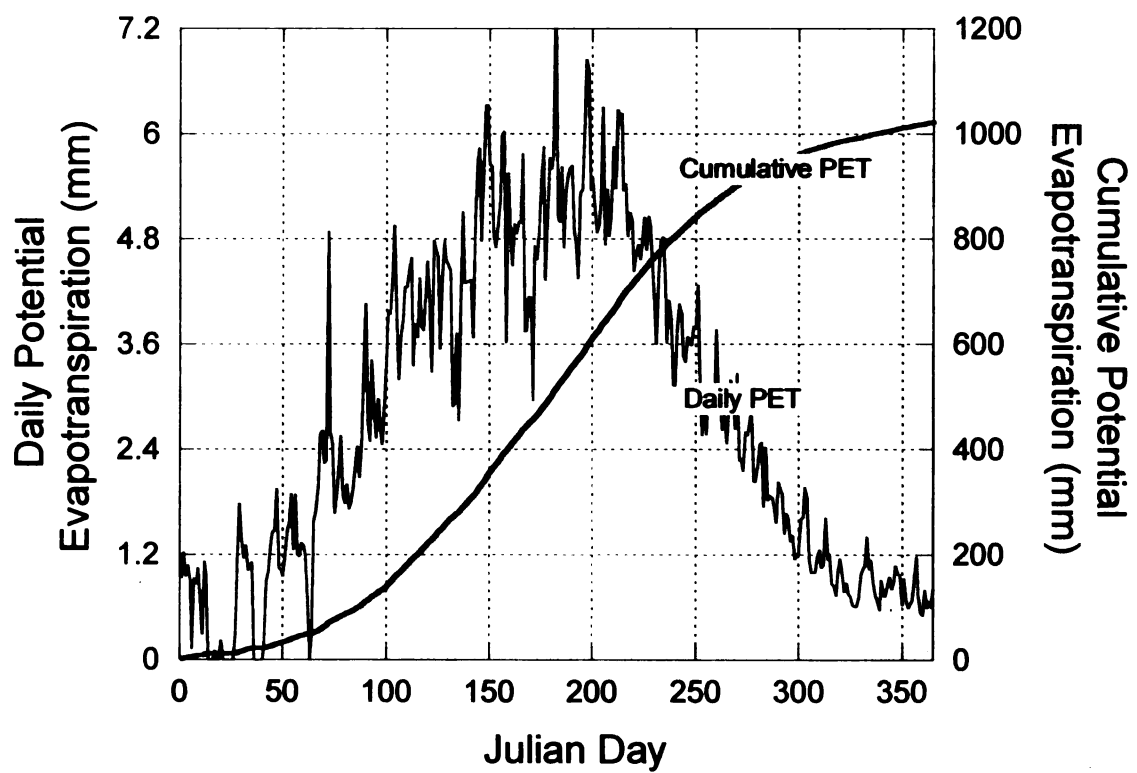


Figure 3-4: Daily and Cumulative PET.

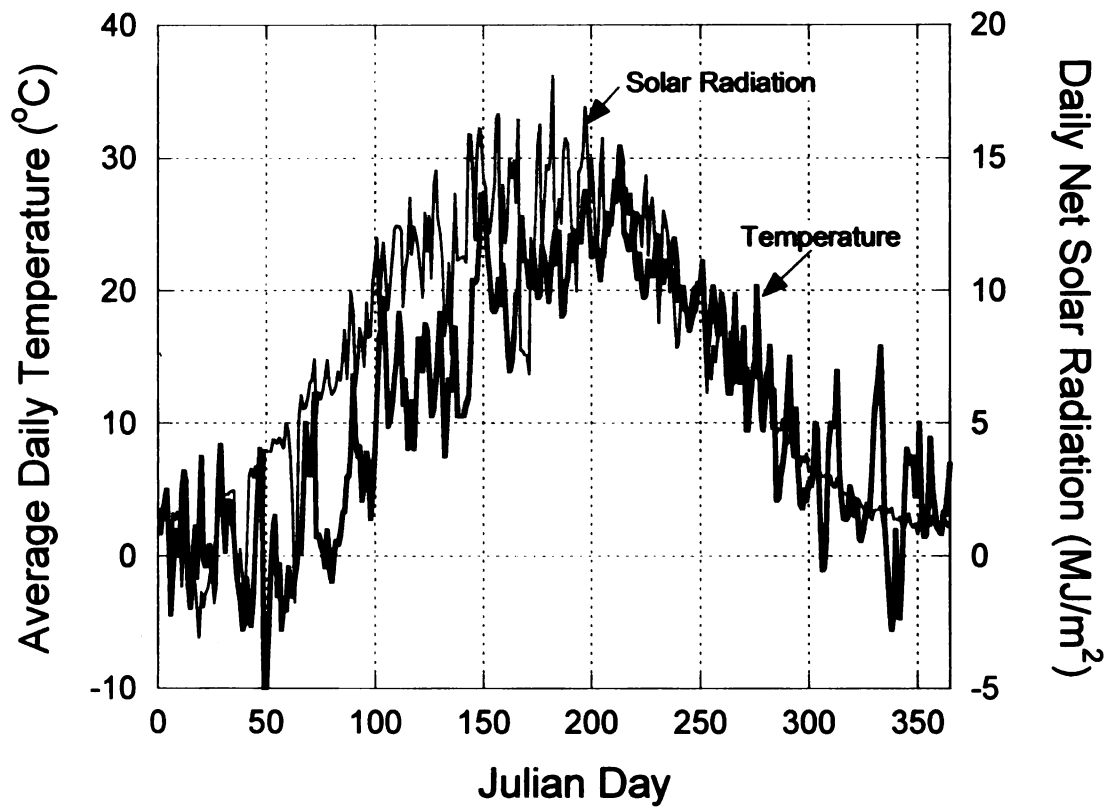


Figure 3-5: Daily Average Temperature and Daily Net Solar Radiation.

### **3.3.4 Boundary Conditions**

Atmospheric boundary conditions were applied for the top boundary (top of the vegetation layer). 365 time-variable boundary records were used correlating to the daily precipitation and PET input for the top boundary. Heat flow and ground freezing was ignored. A free drainage boundary (unit gradient) was assigned to the bottom boundary (Figure 3-1).

### **3.3.5 Time Step, Error Tolerance, Mesh Design, and Initial Conditions**

Time was measured in days with an initial time of 0 and final time of 365 beginning on January 1, 2006 and ending on December 31, 2006. Initial, minimum and maximum time steps were kept constant at  $1 \times 10^{-15}$ ,  $1 \times 10^{-12}$  and 0.5 days, respectively.

The maximum number of iterations was 20, water content tolerance was 0.001 and pressure head tolerance was 0.01 m. HYDRU-2D default values were used for all other iteration criteria.

A rectangular mesh domain was used for all simulations but the vertical discretization of the mesh varied depending on the performance of the simulation. When possible, the number of mesh nodes in the vertical direction was 750 for covers with a waste layer and 200 for the lysimeters. These values were used because increasing the mesh nodes to greater than 750 and 200 when possible made no significant difference in the simulation results. Due to numerical error, some simulations did not run to completion at these mesh sizes. For those situations, the number of vertical nodes was reduced until the simulation ran. A reduction in the number of vertical mesh nodes had a significant effect on the estimated percolation in some cases. This may be due to numerical error. The mesh discretization of each simulation is discussed in Chapter 4.

The initial condition for all soils was set at -10 m of pressure head (suction). Initial pressure head conditions should match the matric suction corresponding to the measured water content of the soil being modeled. In this situation, no real site or soil was being simulated. This initial condition corresponds to a volumetric water content of about 0.25 for all cover soils (Figure 3-2).

### **3.3.6 Fracture Properties**

Parameters regarding the fracture-matrix interface were kept constant at  $w = 0.5$ ,  $\beta = 3$ ,  $\gamma = 0.4$ , and  $a = 1$  for all simulations. The interface hydraulic conductivity,  $K_a$ , was  $1/100^{\text{th}}$  of the soil matrix hydraulic conductivity. When a landfill cover system with preferential flow was being simulated, the fracture hydraulic properties were  $\theta_r = 0.0$ ,  $\theta_s = 0.5$ ,  $\alpha = 0.1 \text{ cm}^{-1}$ ,  $n = 2$ , and  $I = 0.5$ . For all simulations with preferential flow, the hydraulic conductivity of the fracture was kept at 2 cm/s except when this parameter was varied to observe its effect on percolation. These parameters were used by Šimůnek et al. (2003) when preferential flow was simulated. For the simulations when only capillary flow was modeled, the fracture parameters were set equal to the corresponding matrix parameters.

### **3.3.7 HYDRUS-1D**

HYDRUS-1D with dual-permeability option was released after a majority of simulations had been completed in HYDRUS-2D. For this reason, HYDRUS-1D was used to verify a small number of simulations carried out in HYDRUS-2D. Almost all cap simulations and lysimeter without preferential flow simulations produced closely matching results in HYDRUS-1D and HYDRUS-2D. However, simulations of a

lysimeter with preferential flow almost always had difficulty running to completions in HYDRUS-2D. In many cases, the mesh had to be decreased to 75 nodes vertically in order for the simulations to run to completion which probably yielded erroneous results. For this reason, all simulations of a lysimeter with preferential flow were executed in HYDRUS-1D at a mesh of 150. In these simulations, iteration criteria had to be altered so the simulations would run. The water content tolerance was decreased to 0.0001 and the pressure head tolerance was decreased to 0.001 m. The upper limit of the tension interval was increased from 100 m as used in HYDRUS-2D to  $1 \times 10^6$  m. In HYDRUS-1D an additional input parameter regarding the fraction of precipitation that goes into the fracture has been added. This controls how much of the applied precipitation enters directly into the fractures. In HYDRUS-2D, this parameter is referred to as  $q_{TOP}$  but is “hard-coded” and hence cannot be changed easily. The HYDRUS-2D default value of 0.5 was used for all simulations. All other parameters were maintained the same as that used for HYDRUS-2D.

## **CHAPTER 4**

### **RESULTS AND DISCUSSION**

The key objective of this study is to numerically evaluate the effect of various soil and waste hydraulic parameters on the percolation through evapotranspirative landfill covers and lysimeters when preferential flow is present. All simulations were carried out using HYDRUS-2D and HYDRUS-1D. The numerical model simulations are summarized in Table 4-1.

These two key hypotheses were tested in this study: (1) percolation measured using lysimeters does not equate to the percolation across the cover waste boundary because lysimeters exclude the waste layer and evapotranspirative gradients at the interface; and (2) when only capillary flow is considered (and flow through fractures is ignored) percolation is under-estimated. The results of the simulations listed in Table 4-1 are discussed in this chapter.

Table 4-1: Summary of Simulations Carried out Using HYDRUS.

| Parameter Varied      | Simulations |           | TwL (m)             | KvL (cm/s)       | KsL (cm/s)                           | KwL (cm/s)   | KfR (cm/s)       | Fracture Extent | Duration (years) | w                         | q <sub>TOP</sub>          | Corresponding Figure(s) |
|-----------------------|-------------|-----------|---------------------|------------------|--------------------------------------|--|------------------|-----------------|------------------|---------------------------|---------------------------|-------------------------|
|                       | Cap         | Lysimeter |                     |                  |                                      |  |                  |                 |                  |                           |                           |                         |
| Presence of Fractures | 2           | 2         | 6.1                 | 10 <sup>-3</sup> | 10 <sup>-5</sup>                     | 10 <sup>-3</sup>   | 2                | WL              | 2                | 0.5                       | 0.5                       | Fig. 4-1<br>Fig. 4-2    |
| Fracture Extent       | 6           | 4         | 6.1                 | 10 <sup>-3</sup> | 10 <sup>-5</sup>                     | 10 <sup>-3</sup>   | 2                | VL<br>SL<br>WL  | 1                | 0.5                       | 0.5                       | Fig. 4-4<br>Fig. 4-5    |
| KfR                   | 3           | 3         | 6.1                 | 10 <sup>-3</sup> | 10 <sup>-5</sup>                     | 10 <sup>-3</sup><br>10 <sup>-4</sup><br>10 <sup>-4</sup> | 0.02<br>0.2<br>2 | WL              | 1                | 0.5                       | 0.5                       | Fig. 4-6                |
| w                     | 3           | 1         | 6.1                 | 10 <sup>-3</sup> | 10 <sup>-5</sup>                     | 10 <sup>-3</sup>   | 2                | WL              | 1                | 0.5<br>0.2<br>0.1<br>0.05 | 0.5                       | Fig. 4-7                |
| q <sub>TOP</sub>      | 4           | 4         | 6.1                 | 10 <sup>-3</sup> | 10 <sup>-5</sup>                     | 10 <sup>-3</sup>   | 2                | WL              | 1                | 0.5                       | 0.5<br>0.2<br>0.1<br>0.05 | Fig. 4-8<br>Fig. 4-9    |
| KsL                   | 6           | 6         | 6.1                 | 10 <sup>-3</sup> | 10 <sup>-5</sup><br>10 <sup>-6</sup> | 10 <sup>-3</sup>   | 2                | WL              | 1                | 0.5                       | 0.5                       | Fig. 4-10               |
| KwL                   | 3           | 3         | 6.1                 | 10 <sup>-3</sup> | 10 <sup>-5</sup>                     | 10 <sup>-3</sup><br>10 <sup>-4</sup><br>10 <sup>-5</sup> | 2                | WL              | 1                | 0.5                       | 0.5                       | Fig. 4-11<br>Fig. 4-12  |
| TwL                   | 3           | 3         | 3.05<br>6.1<br>12.2 | 10 <sup>-3</sup> | 10 <sup>-5</sup>                     | 10 <sup>-3</sup>   | 2                | WL              | 1                | 0.5                       | 0.5                       | Fig. 4-13               |

Note: 1. VL = Vegetation Layer; SL = Storage Layer; WL = Waste Layer; FR = Fracture; and T = Thickness.

2. TvL = 0.3 m and T<sub>SL</sub> = 1 m for all simulations.

3. Meteorological data collected in 2006 was used for all simulations and was repeated for 2 year simulations.

4. Pressure head equal to -10 m was used for all simulations as the initial condition.

5. Water content tolerance of 0.001 or 0.0001 and pressure head tolerance of 0.01 m or 0.001 m was used for all simulations.

#### **4.1 PRESENCE OR ABSENCE OF FRACTURES**

Four simulations were executed in HYDRUS to evaluate the effect of capillary flow only versus capillary and preferential flow. These simulations represent a time period of two years. The simulated cumulative percolations versus time are shown in Figure 4-1.

All simulations have a hydraulic conductivity of  $10^{-3}$  cm/s and  $10^{-5}$  cm/s for the vegetation layer and storage layer, respectively. Cap simulations included a waste layer having a hydraulic conductivity of  $10^{-3}$  cm/s. All simulations have a waste layer thickness of 6.1 m when present. When preferential flow was simulated, fractures extended through the waste layer for the cap simulations and through the storage layer for the lysimeter simulations. Vertical discretization of mesh nodes was 750 for the cap with no preferential flow and 600 for the cap with preferential flow. 200 mesh nodes were used for the lysimeter without preferential flow and 150 for the lysimeter with preferential flow. Simulations in HYDRUS-2D for the lysimeter with preferential flow contained unrealistic results of upward cumulative percolation which was attributed to numerical error and therefore were repeated in HYDRUS-1D. To demonstrate the accuracy between the two HYDRUS versions, the simulation of the cap with preferential flow was also repeated in HYDRUS-1D and produced similar results as seen in Figure 4-1 along with the results of the other four simulations. The water balance error for the simulations was negligible ( $< 0.1\%$ ) for the lysimeters and approximately 27% for the cap, which is relatively high.

To insure that simulation width does not affect percolation, selected simulations were repeated with a width of 1 cm. These simulations confirmed that simulation width is a non-influential parameter.

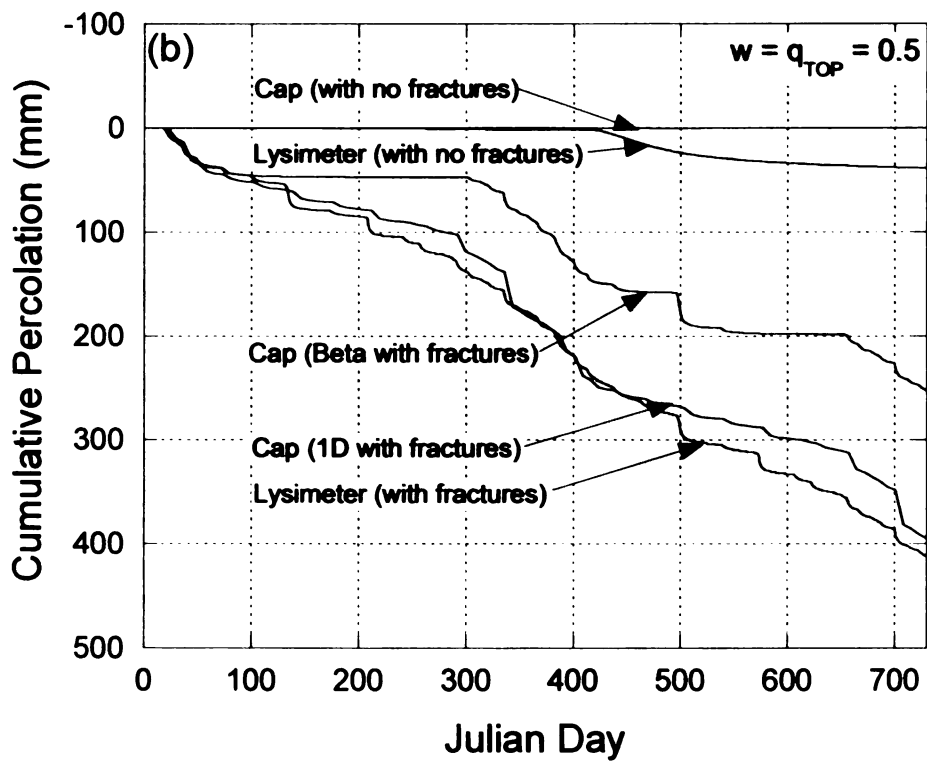
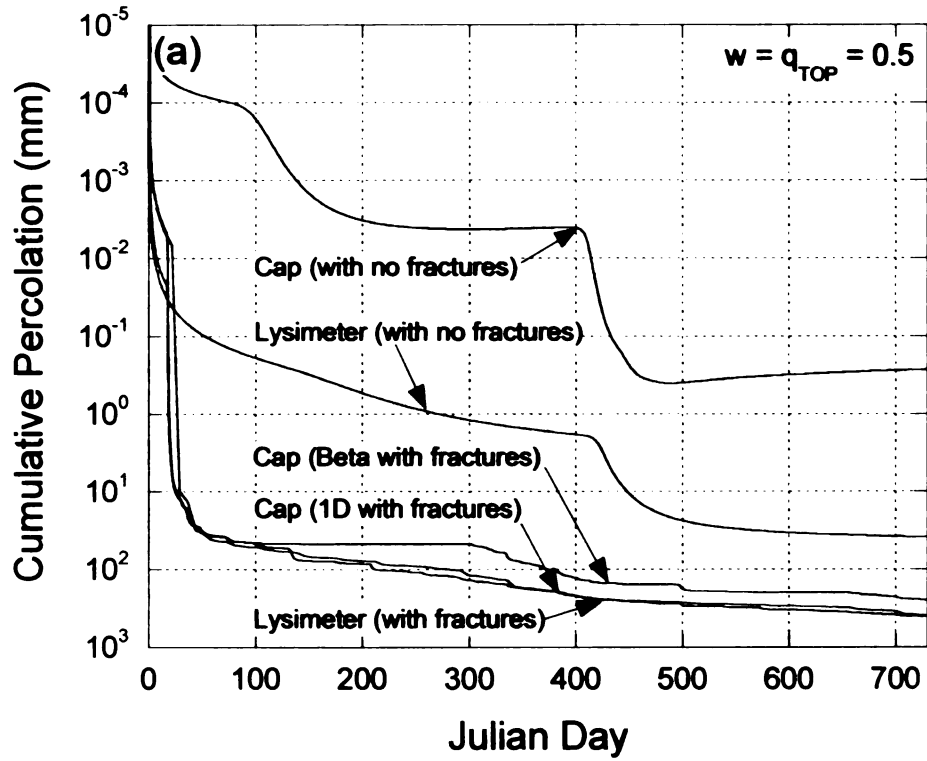


Figure 4-1: Simulated Percolation through Cap versus Lysimeter with and without Preferential Flow on a Log Scale (a); and Linear Scale (b).

Figure 4-1 shows that percolation follows a cyclical pattern each year when only capillary flow is considered. In the cases with preferential flow, a cyclical pattern was not observed. Figure 4-1b plots the same cumulative percolation of Figure 4-1a on a linear scale to confirm that a cyclical pattern was not observed when preferential flow was present. Figure 4-1 also illustrates that the lysimeter without preferential flow had percolation that was about two orders of magnitude higher compared to the cap without preferential flow. However, once preferential flow was introduced, percolation increased as hypothesized but with no significant difference in percolation between the lysimeter and cap. For the remaining simulations, simulation length was reduced to one year due to time constraints.

The cumulative evaporation and runoff and the cumulative percolation through the bottom most boundary of the four simulations are presented in Figure 4-2. The cap and lysimeter with no preferential flow have the same amount of cumulative evaporation and runoff because the infiltrating water is being stored in the storage layer of the evapotranspirative cover as it is designed to do. They also have the highest amount of cumulative evaporation and runoff because they lack preferential flow which carries water away from the surface at a much faster rate than the surrounding soil matrix. The cap with preferential flow has the second most cumulative evaporation and runoff. This is because the preferential flow moves the water to deeper depths reducing direct evaporation and runoff than the cap and lysimeter without preferential flow. It has more cumulative evaporation and runoff than the lysimeter with preferential flow because water is allowed to be stored in the waste layer and later be removed by evaporation.

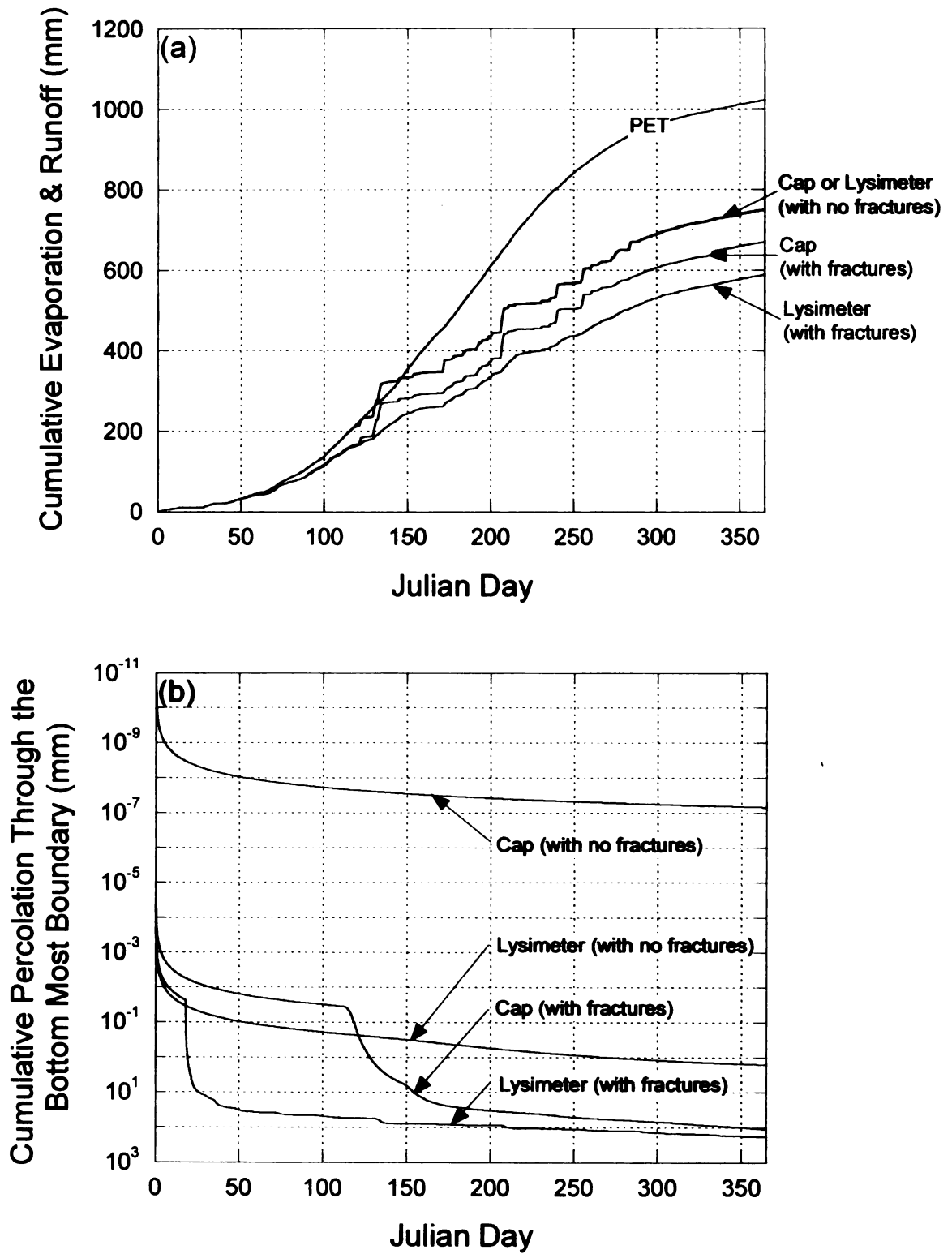


Figure 4-2: Simulated Cumulative Evaporation and Runoff (a); and Simulated Cumulative Percolation through the Bottom Most Boundary (b).

The lysimeter lacks the waste layer and all water passing through the storage layer is immediately removed from the system.

The cumulative percolation through the bottom most boundary, the storage layer for the lysimeter and waste layer for the cap, is presented in Figure 4-2. These percolation amounts follow a similar trend as the percolation in Figure 4-1. The differences in percolation among the simulations can be attributed to the same reasons mentioned in regards to the cumulative evaporation and runoff.

## **4.2 FRACTURE PROPERTIES**

Parameters specific to the pathways of preferential flow, such as the depth through which they extend, the hydraulic conductivity of the fractures, the volume of fractures, and the fraction of surface flow entering the fractures can also have an effect on the amount of percolation into the waste layer. Hence, the effect of fracture depth, fracture hydraulic conductivity, fracture volume, and the amount of surface flow entering the fractures were evaluated.

### **4.2.1 Fracture Depth**

The depth of fractures or preferential flow paths, although difficult to assess in the field, can influence percolation into the waste. For the lysimeter, fracture depth was simulated to extend through the vegetation layer, the vegetation layer and half way through the storage layer, and through the entire vegetation and storage layer. For the cap, fracture depth was simulated to extend through the vegetation layer, the entire vegetation and storage layer, one third of the way into the waste layer, two thirds into the waste layer, and through the entire model profile. The effect of fracture depth is illustrated in Figure 4-3. Although HYDRUS simulates a continuous network of fractures

rather than individual fractures, Figure 4-3 shows the fractures as one large individual fracture for illustration purposes only.

Figure 4-4 represents cumulative percolations from ten simulations showing the affect of preferential flow depth on percolation. All simulations were carried out with a hydraulic conductivity of  $10^{-3}$  cm/s and  $10^{-5}$  cm/s assigned to the vegetation layer and storage layer, respectively. Cap simulations included a waste layer having a hydraulic conductivity of  $10^{-3}$  cm/s. A waste layer thickness of 6.1 m was used in all cap simulations. Preferential flow networks were assigned a hydraulic conductivity of 2 cm/s. Vertical discretization of mesh nodes was 600 for all cap simulations and 150 for lysimeter simulations. The water balance error for the simulations was negligible ( $< 0.1\%$ ) for the lysimeters and approximately 22% for the cap.

A noticeable pattern emerges in Figure 4-4 for both the lysimeter and cap simulations. As preferential flow depth increases, so does the amount of percolation. This occurs because preferential flow carries infiltrating water to deeper depths at faster rates than the surrounding capillary pore matrix. The deeper the preferential flow, the faster the water is carried towards or across the storage layer-waste layer boundary where percolation is assessed. These results indicate that the effectiveness of the storage layer to store the infiltration and reduce percolation is impaired as the depth of preferential flow networks increase.

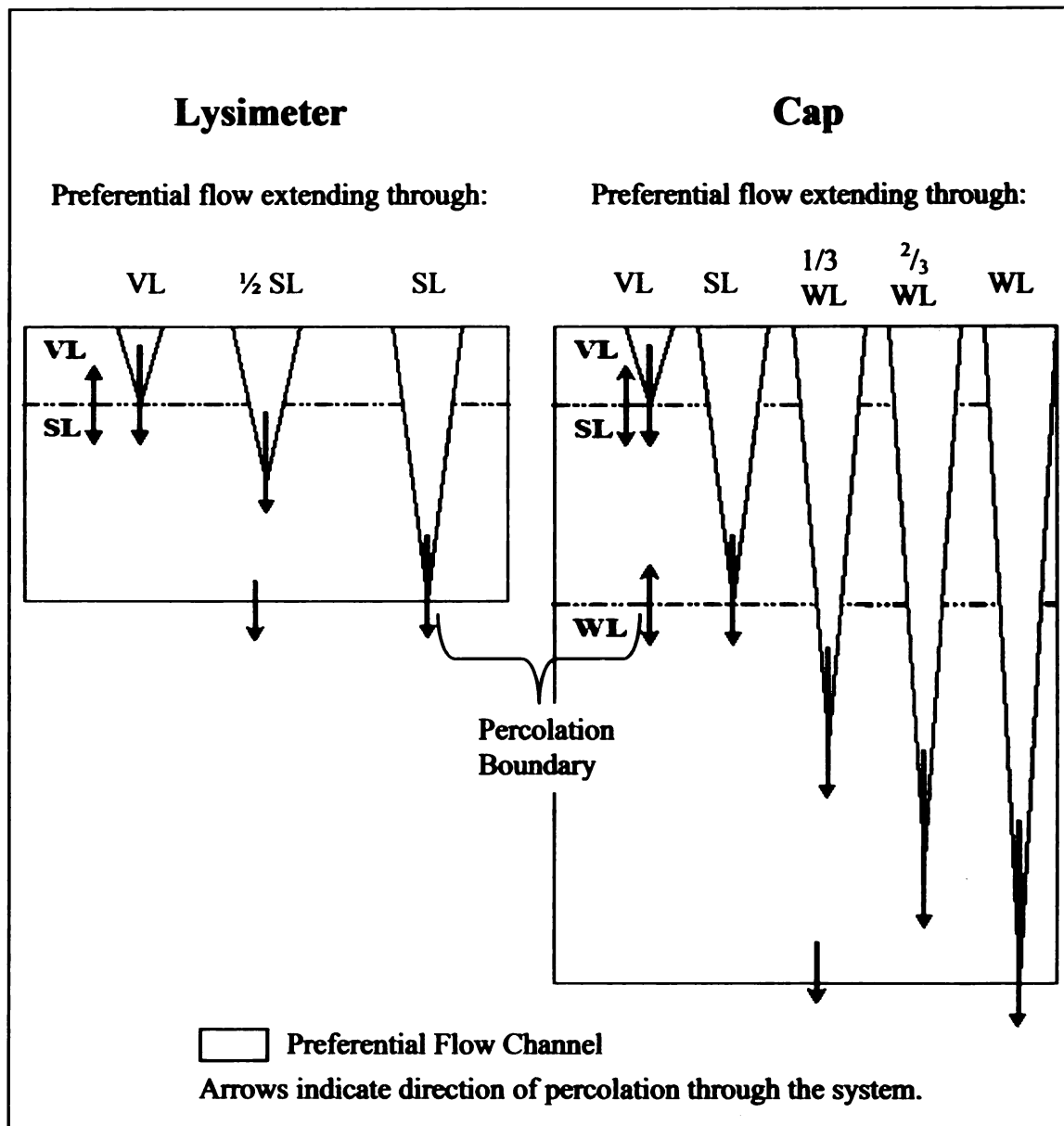


Figure 4-3: Depth of Preferential Flow through Lysimeter and Cap.

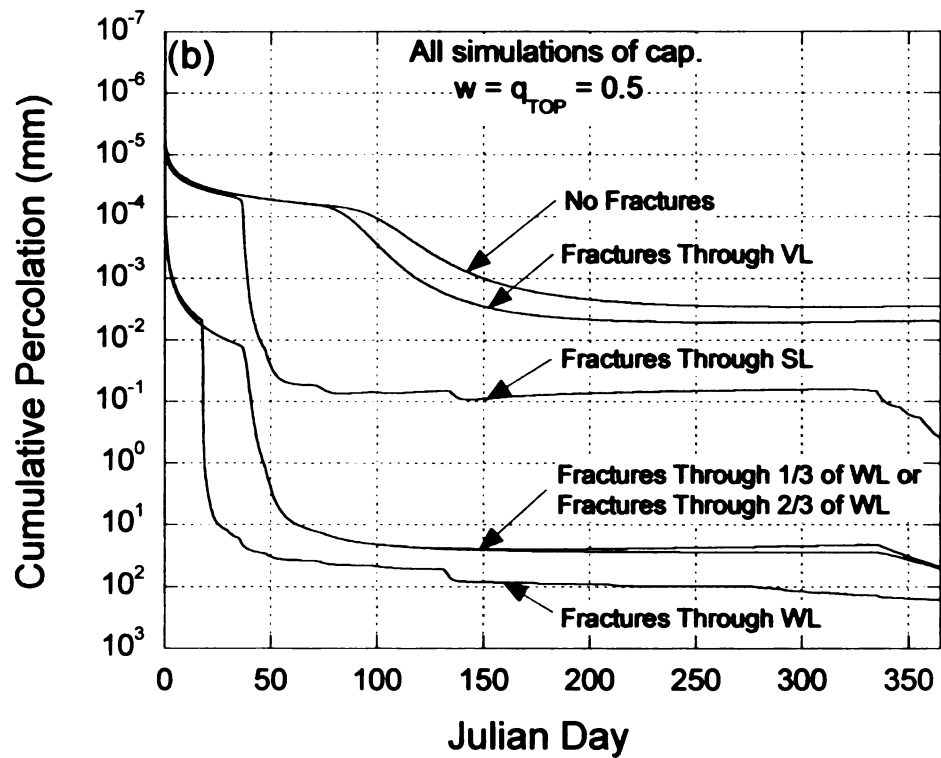
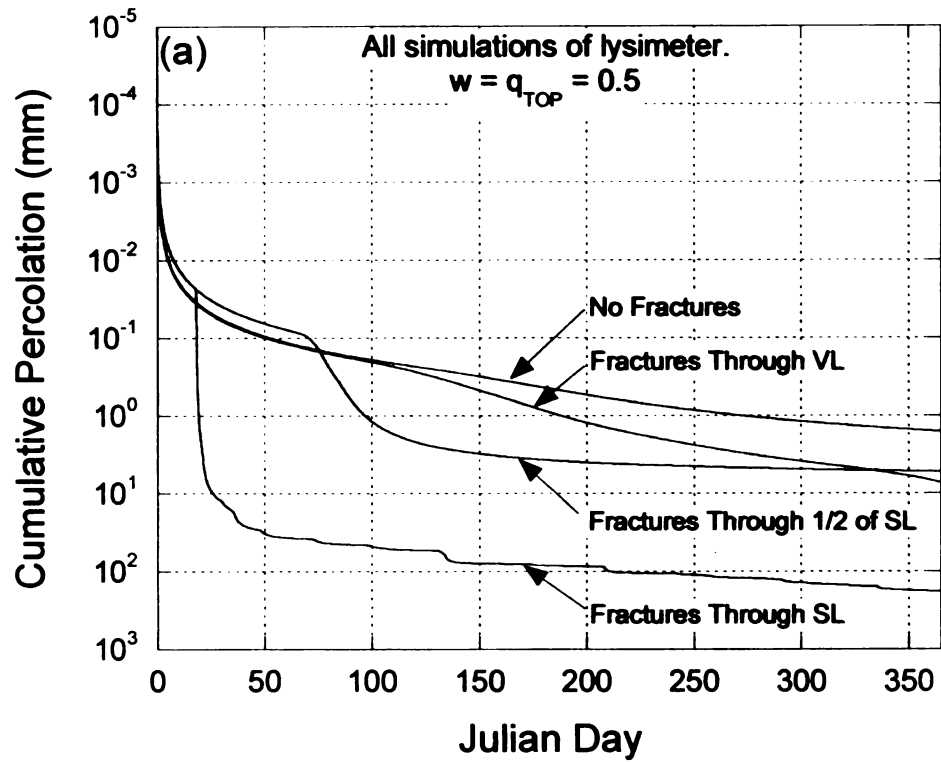


Figure 4-4: Effect of Fracture Depth on Simulated Percolation for Lysimeter (a); and Cap (b).

To insure that the results were not just a product of the layer's soil water characteristic properties, the waste layer hydraulic conductivity was decreased from  $10^{-3}$  cm/s to  $10^{-4}$  cm/s. It can be seen in Figure 4-5 that despite the change in waste layer hydraulic conductivity, a similar pattern in percolation was observed. Regardless of the soil and waste matrix hydraulic properties, percolation increases as the depth of the fracture network increases.

#### **4.2.2 Hydraulic Conductivity of Fractures**

A second parameter specific to the pathways of preferential flow is the hydraulic conductivity of the fractures. Because HYDRUS simulates preferential flow by representing the fracture network as a separate material, a hydraulic conductivity is required to model the rate of water flow through the system. Six simulations were executed, three for a cap and three for a lysimeter, with three different fracture hydraulic conductivities. The results are displayed in Figure 4-6.

Three fracture hydraulic conductivities, 2 cm/s, 0.2 cm/s, and 0.02 cm/s, were applied to the cap and lysimeter simulations. All simulations were carried out with hydraulic conductivity equal to  $10^{-3}$  cm/s and  $10^{-5}$  cm/s assigned to the vegetation layer and storage layer, respectively. Cap simulations had a waste layer with a hydraulic conductivity of  $10^{-3}$  cm/s and a waste layer thickness of 6.1 m. Fractures extended through the waste layer in the cap and through the storage layer in the lysimeter. 750 mesh nodes were used to discretize the cap and 150 for the lysimeter. The water balance error for the simulations was negligible ( $< 0.1\%$ ) for the lysimeters and approximately 20% for the cap.

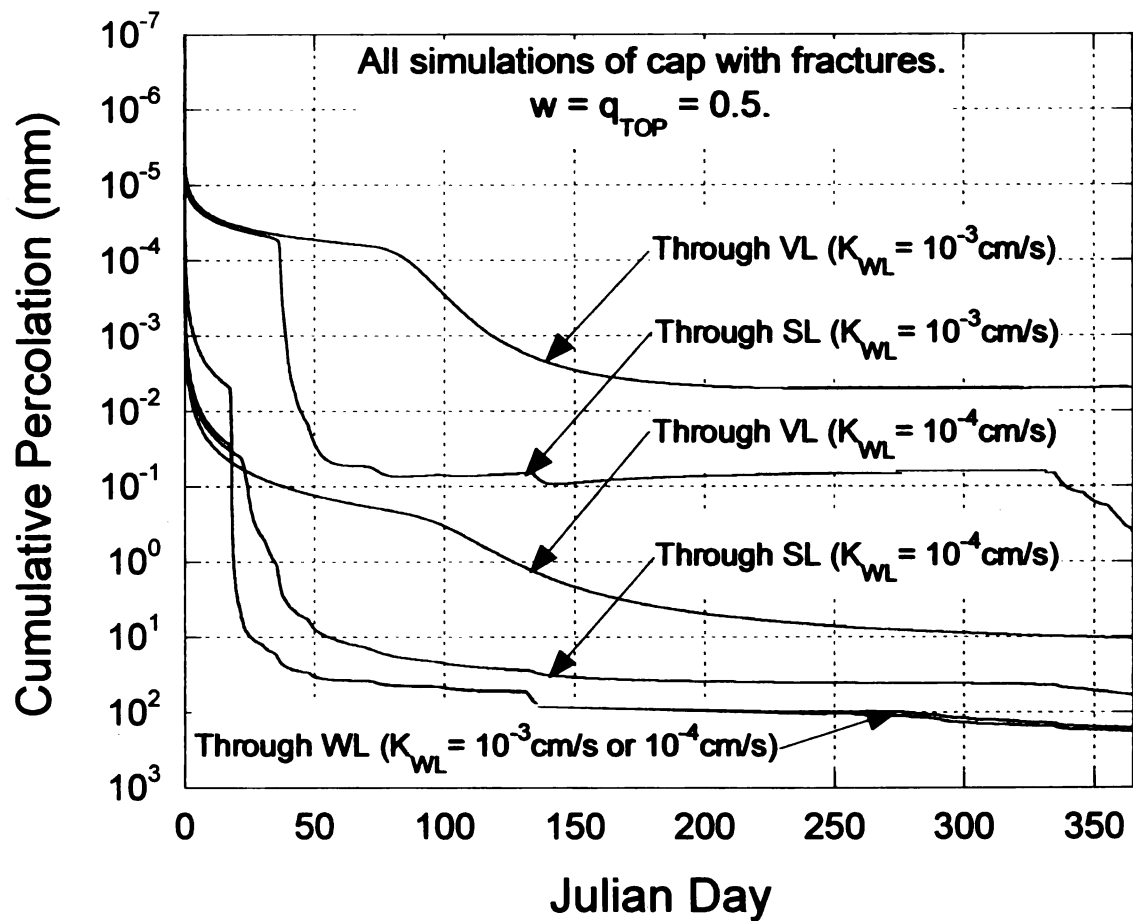


Figure 4-5: Effect of Waste Layer Hydraulic Conductivity and Fracture Depth on Simulated Percolation.

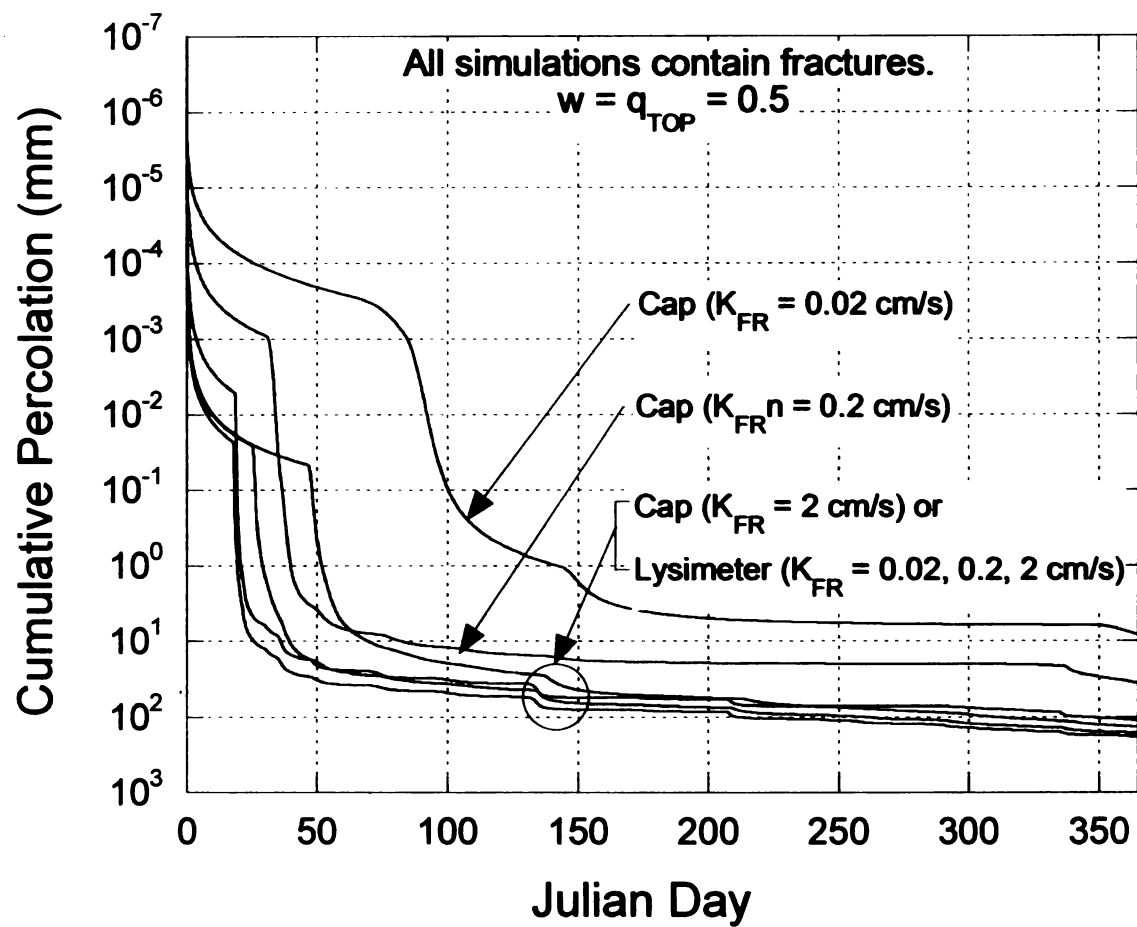


Figure 4-6: Effect of Hydraulic Conductivity of Fractures on Simulated Percolation.

Figure 4-6 shows that the hydraulic conductivity of the fractures affects the percolation by a significant amount for the cap. For the cap simulations, percolation decreases as the hydraulic conductivity of the fracture network decreases. For the lysimeter simulations, the hydraulic conductivity of the fractures had little effect on the percolation. The length of travel through fractures for infiltrated water in the lysimeter is relatively small compared to that for the cap. Hence, for a given fracture conductivity the percolation through the lysimeter is greater than that through the cap.

#### **4.2.3 Volume of Fractures**

The ratio of the volume of the fracture domain to the total volume of the system ( $w$ ) is an important parameter because it controls the relative proportions of preferential flow versus capillary flow in the soil profile. To evaluate the effect of volume of fractures, eight simulations were carried out with varying  $w$ .

$w$  was varied (0.5, 0.2, 0.1 and 0.05) in eight simulation and the results are presented in Figures 4-7. All simulations used a hydraulic conductivity of  $10^{-3}$  cm/s and  $10^{-5}$  cm/s for the vegetation layer and storage layer, respectively. Cap simulations included a waste layer having a hydraulic conductivity of  $10^{-3}$  cm/s with a waste layer thickness of 6.1 m. Fractures extended through the waste layer in the cap and through the storage layer in the lysimeter. The hydraulic conductivity for the fractures was assigned 2 cm/s. Vertical discretization of mesh nodes was 600 for the cap except, when  $w$  was 0.05, the mesh was 500. Vertical discretization of mesh nodes was 150 for the lysimeter. The water balance error for the simulation was negligible ( $<0.1\%$ ) for the lysimeters and approximately 16% for the cap.

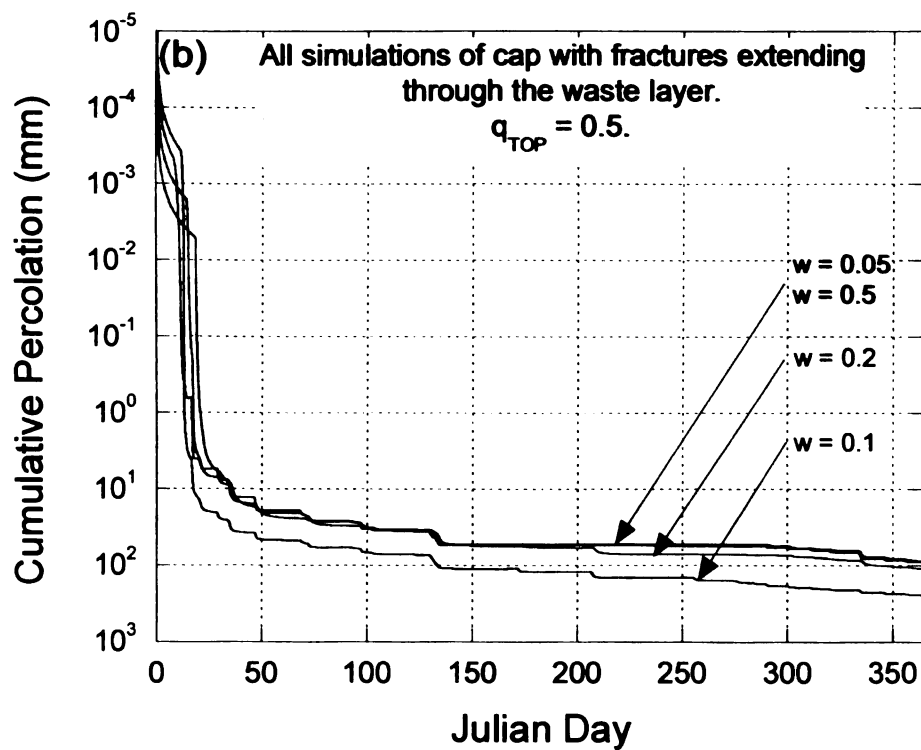
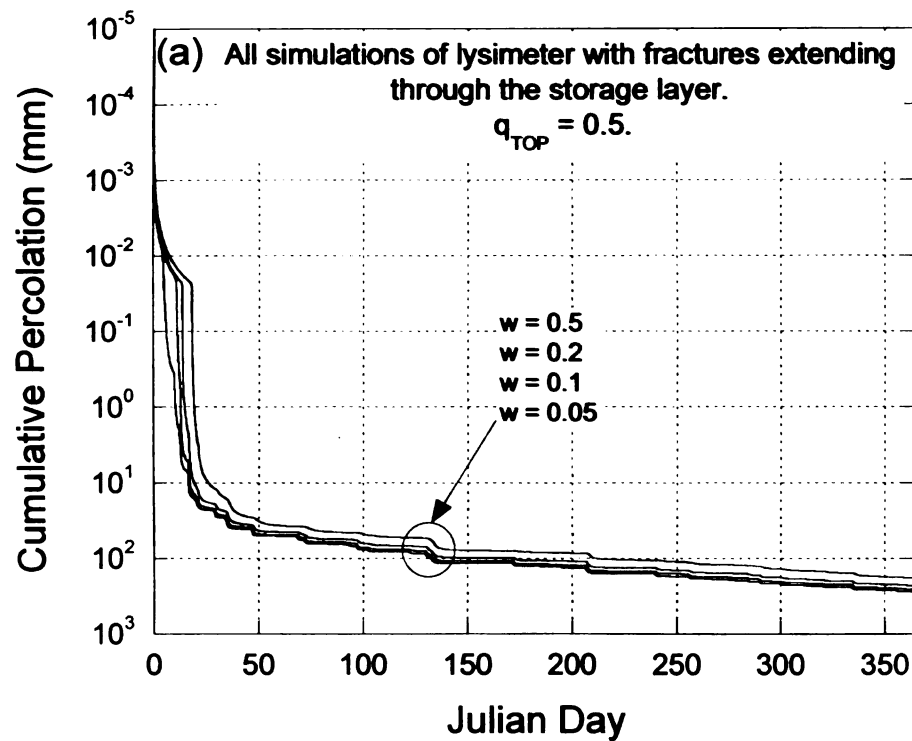


Figure 4-7: Simulated Effect of the Volume of Fractures on Percolation for Lysimeter (a); and Cap (b).

From these simulations, it was observed that the ratio of the volume of the fractures to the total volume of the system can influence percolation. For both the lysimeter and cap, the larger the fracture domain, the less cumulative percolation. The only exception being when  $w$  is 0.05 for the cap. This simulation seems to vary from the pattern seen in the other seven simulations and is probably due to the coarser mesh size used for that particular simulation which may have reduced the accuracy of the results. It should be noted that  $q_{TOP}$ , the fraction of surface flow entering into the fracture network, was maintained at 0.5 for every value of  $w$  so even as the amount of fractures changed, the amount of water entering into the fractures remained the same. The unchanging  $q_{TOP}$  value might be the reason for the unexpected results of these simulations.

#### **4.2.4 Effect of Fraction of Surface Flow Entering Fractures**

The fraction of surface flow entering directly into the fracture domain ( $q_{TOP}$ ) is a fourth fracture property that could potentially affect the amount of percolation.  $q_{TOP}$  was varied in eight simulations and the results are displayed in Figure 4-8.

$q_{TOP}$  was varied between 0.5, 0.2, 0.1 and 0.05.  $w$  remained constant at 0.5 in all simulations. For all simulations, hydraulic conductivities equal to  $10^{-3}$  cm/s and  $10^{-5}$  cm/s were assigned for the vegetation layer and storage layer, respectively. Cap simulations included a waste layer having a hydraulic conductivity of  $10^{-3}$  cm/s. All simulations have a waste layer thickness of 6.1 m, when present. Fractures extended through the waste layer in the cap and through the storage layer in the lysimeter. The hydraulic conductivity for the fractures was assigned 2 cm/s. Vertical discretization of mesh nodes was 750 for the cap except when  $q_{TOP}$  was 0.05 the mesh was 600. The mesh was 75 for all lysimeter

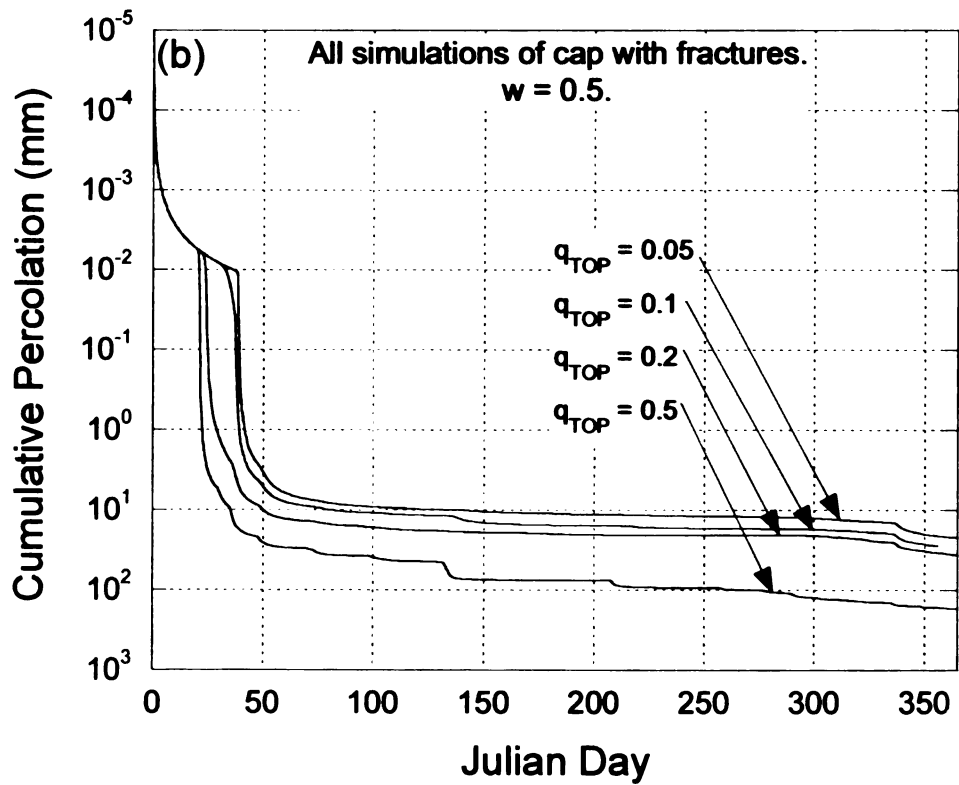
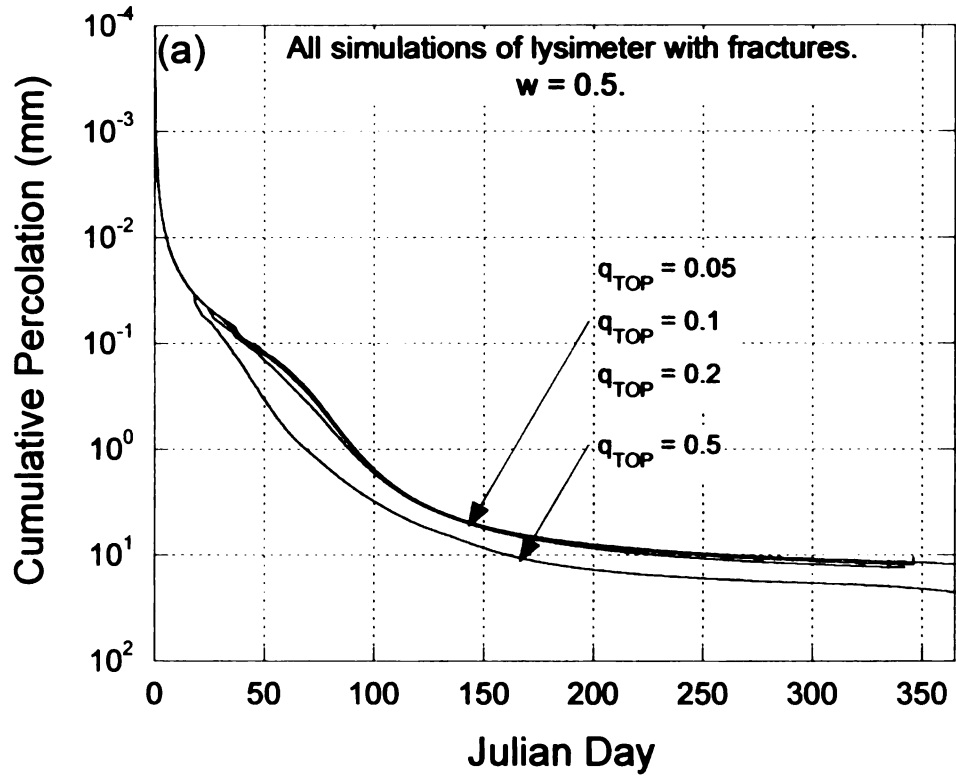


Figure 4-8: Simulated Effect of  $q_{TOP}$  for a Lysimeter (a); and Cap (b).

simulations and were completed in HYDRUS-2D because they would not run in HYDRUS-1D once  $q_{TOP}$  was changed. The water balance error for the simulations was negligible ( $< 0.1\%$ ) for the lysimeter and approximately 20% for the cap.

As seen in Figure 4-8,  $q_{TOP}$  has a greater effect on percolation in the cap than in the lysimeter. In the cap simulations, percolation increases as  $q_{TOP}$  increases. Figure 4-9 illustrates the effect on percolation when  $w$  and  $q_{TOP}$  are varied together. In these simulations, as  $w$  and  $q_{TOP}$  increase so does the percolation as expected.

### **4.3 HYDRAULIC CONDUCTIVITY OF STORAGE LAYER**

Design properties of the evapotranspirative cover also influence the amount of percolation into the waste layer. Here the hydraulic conductivity of the storage layer was varied in 12 simulations to demonstrate its effect on percolation and the results are displayed in Figure 4-10.

Three storage layer hydraulic conductivities ( $10^{-4}$  cm/s,  $10^{-5}$  cm/s, and  $10^{-6}$  cm/s) were applied to the cap and lysimeter, with and without preferential flow. All simulations have a vegetation layer with a hydraulic conductivity equal to  $10^{-3}$  cm/s and cap simulations have a waste layer with a hydraulic conductivity equal to  $10^{-3}$  cm/s. All cap simulations have a waste layer with a thickness of 6.1 m. When preferential flow was simulated, fractures extend through the waste layer in the cap and through the storage layer in the lysimeter with a hydraulic conductivity of 2 cm/s. Vertical discretization of mesh nodes was 750 for the cap except when the storage layer hydraulic conductivity was  $10^{-6}$  cm/s the mesh was reduced to 250 in order for the simulation to run.

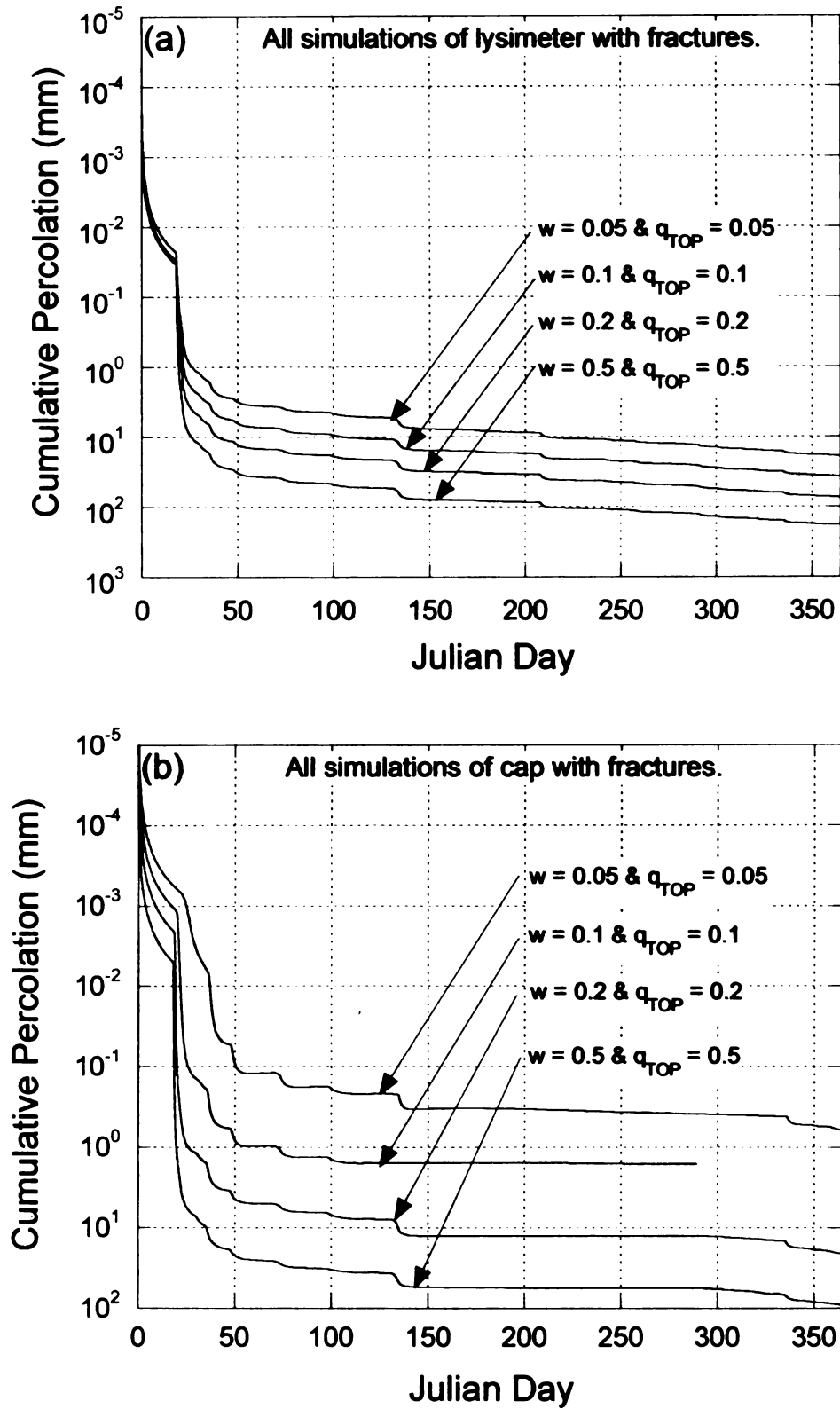


Figure 4-9: Simulated Effect of  $w$  and  $q_{TOP}$  on Percolation through a Lysimeter (a); and Cap (b).

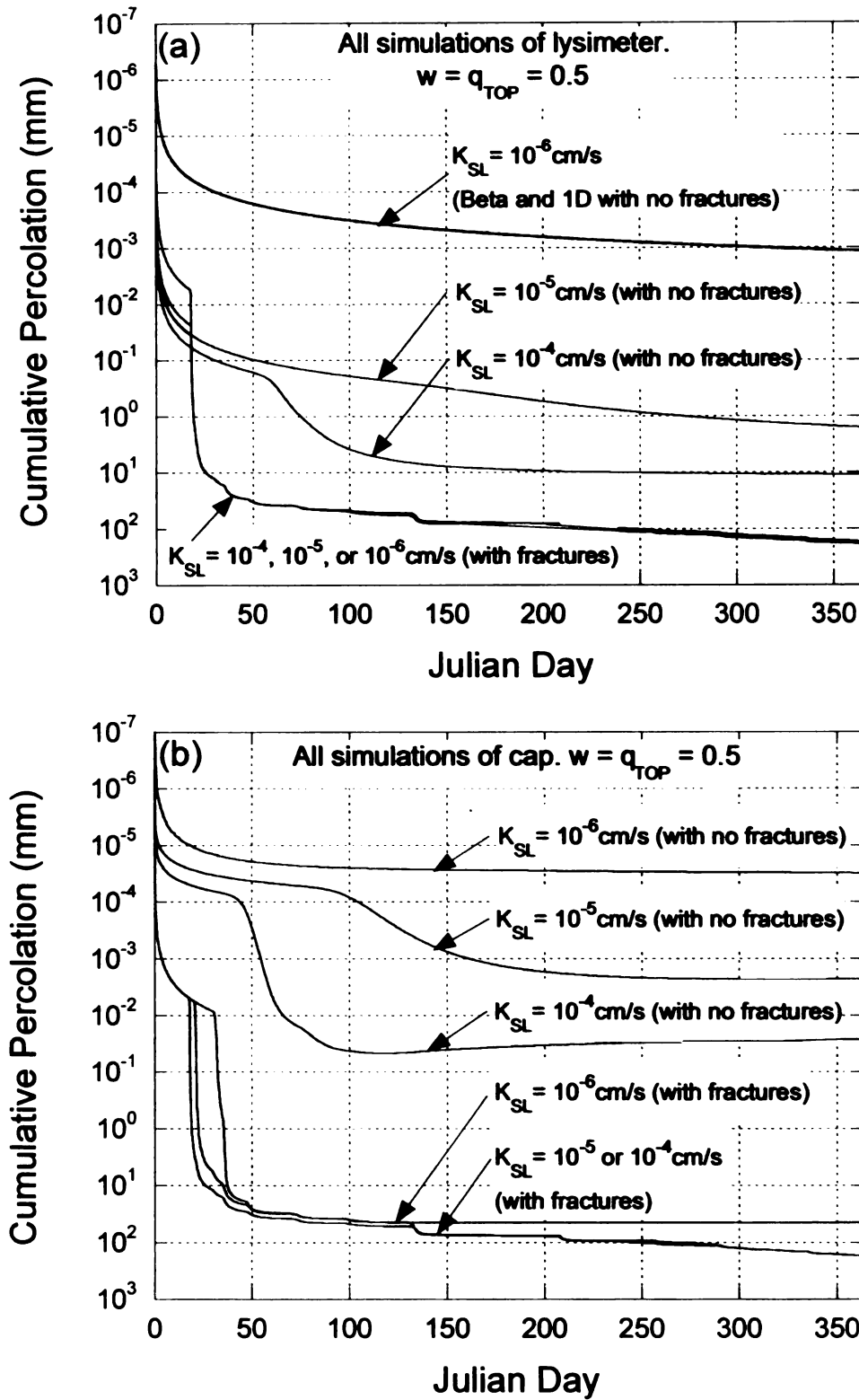


Figure 4-10: Effect of Hydraulic Conductivity of the Storage Layer on Simulated Percolation of Lysimeter (a); and Cap (b).

Vertical discretization of mesh nodes was 150 for the lysimeter except when the storage layer hydraulic conductivity was  $10^{-6}$  cm/s the mesh was reduced to 25 in order for the simulation to run. The cap simulation with a storage layer hydraulic conductivity of  $10^{-6}$  cm/s and no preferential flow was also ran in HYDRUS-1D as a check to insure the two HYDRUS programs produce the same results. The water balance error was negligible ( $<0.1\%$ ) for simulations ran in HYDRUS-1D and approximately 30% for the remaining cap simulations.

As seen in Figure 4-10, when preferential flow is absent, percolation decreases as the hydraulic conductivity of the storage layer decreases. This is expected because the lower the hydraulic conductivity, the more restricted the water flow through the layer. Once preferential flow is simulated, percolation is just over 100 mm for all three storage layer hydraulic conductivities. This happens because the water has a direct route through the preferential flow pathways to the bottom of the storage layer. Hence, the percolation is independent of the hydraulic conductivity of the matrix of the storage layer when preferential flow is significant.

#### **4.4 WASTE LAYER PARAMETERS**

Waste layer parameters can influence percolation even though it is not part of the cover system (Khire and Mijares 2008). The hydraulic conductivity and soil-water retention properties of the waste layer and its thickness are parameters that could potentially affect percolation and were explored in the simulations in Figure 4-11.

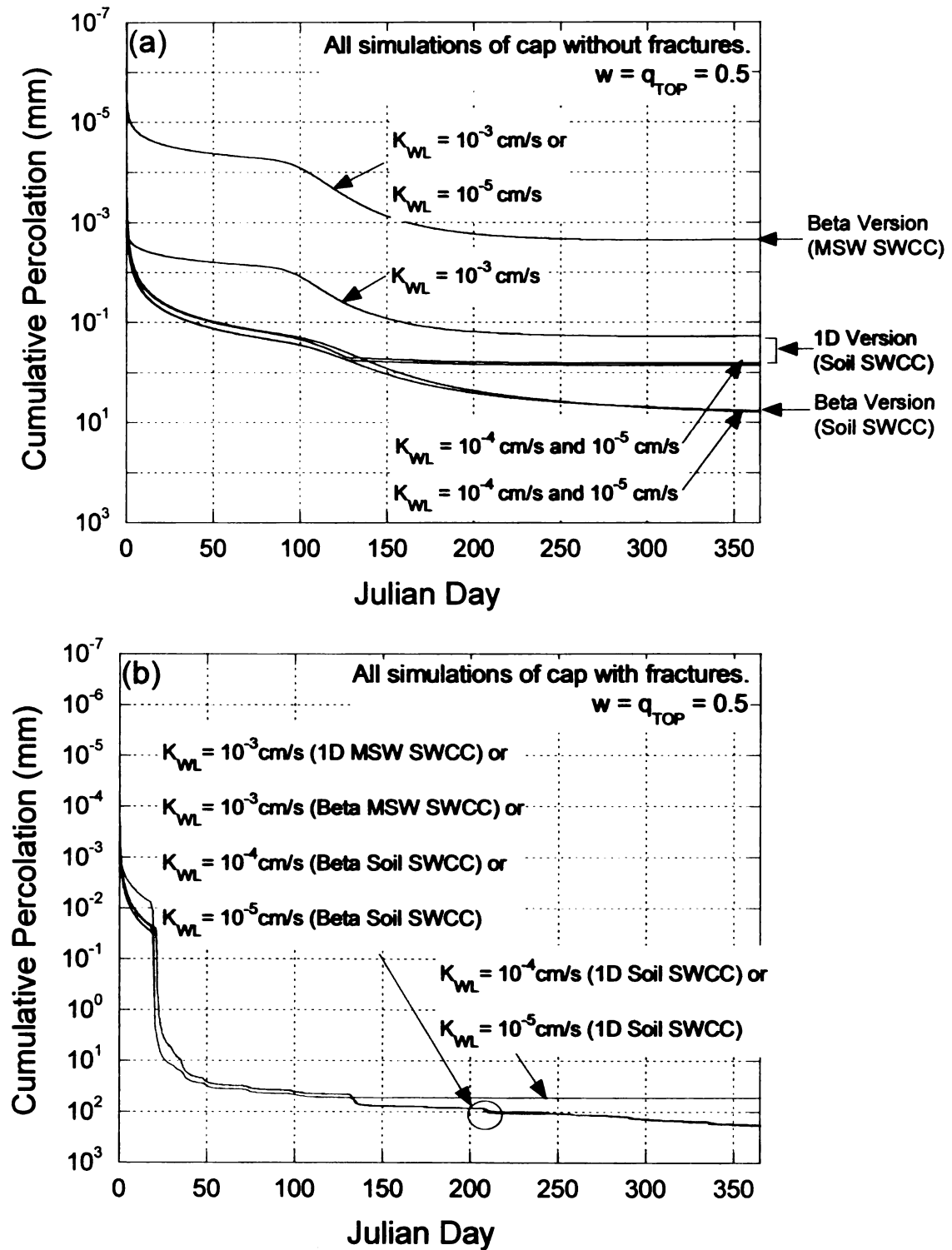


Figure 4-11: Simulated Effect of Hydraulic Conductivity of Waste Layer on Cap Percolation without Preferential Flow (a); and with Preferential Flow (b).

#### 4.4.1 Hydraulic Conductivity of Waste Layer

Six simulations were used to illustrate the effect the waste layer hydraulic conductivity has on percolation. Because the cap simulation results were not as expected, all three simulations were repeated in HYDRUS-1D and are discussed below.

Three waste layer hydraulic conductivities ( $10^{-3}$  cm/s,  $10^{-4}$  cm/s, and  $10^{-5}$  cm/s) were input for the waste layer of the cap with and without preferential flow. Hydraulic conductivity of the vegetation layer and storage layer were input equal to  $10^{-3}$  cm/s and  $10^{-5}$  cm/s, respectively. The simulated waste layer thickness was 6.1 m. When preferential flow was simulated, fractures (hydraulic conductivity = 2 cm/s) extended through the waste layer. Vertical discretization of mesh nodes was 750 for all simulations in both versions of HYDRUS. The water balance error was negligible (<0.1%) for simulations ran in HYDRUS-1D, approximately 30% for simulations ran in HDYRUS-2D without fractures, and approximately 21% for simulations ran in HYDRUS-2D with fractures

Figure 4-11 shows that when preferential flow is absent, the largest waste layer hydraulic conductivity,  $10^{-3}$  cm/s, has the least amount of percolation. The HYDRUS-1D simulations produced similar results. Even though the amount of percolation produced by the  $10^{-3}$  cm/s waste layer varies between the two HYDRUS versions, they both show that the greater the waste layer hydraulic conductivity the smaller the amount of percolation. Because these results are not intuitive, simulations were repeated using the van Genuchten-Mualem single-porosity modeling option as opposed to the dual-permeability modeling option. The simulations using the van Genuchten-Mualem single-porosity modeling option produced the same trend but are not shown in Figure 4-11. One possible

explanation is the contrast in hydraulic conductivities between the storage and waste layer. The storage layer has a hydraulic conductivity of  $10^{-5}$  cm/s so the larger the hydraulic conductivity of the waste layer, the larger the contrast in the soil-water retention properties between the two. This may be producing an effect that is similar to a capillary barrier. The water in the storage layer can not move into the waste layer until a water-entry matric suction is reached (Fig. 1-3). As the waste layer hydraulic conductivity decreases, it more closely matches that of the storage layer so the water-entry matric suction is reached more quickly allowing water to infiltrate into the waste layer. A second explanation may be the effect of the waste layer SWCC. For a waste layer hydraulic conductivity of  $10^{-3}$  cm/s, an SWCC developed by Benson and Wang (1998) representing MSW was applied (Table 3-1). When the waste layer hydraulic conductivity was  $10^{-4}$  cm/s and  $10^{-5}$  cm/s, SWCCs of soils with the same hydraulic conductivity were applied because there is very little published data on MSW SWCCs as the hydraulic conductivity of the MSW decreases when the waste settles and undergoes decomposition. The assumption that SWCC of MSW resembles that of an equivalent soil when the waste has undergone degradation may not be realistic.

In order to demonstrate the effect the waste layer SWCC may have on the percolation, the simulation with a waste layer hydraulic conductivity of  $10^{-5}$  cm/s was repeated with the MSW SWCC. As shown in Figure 4-11, this had a significant effect on the percolation demonstrating that waste layer SWCCs can greatly influence simulated percolation. Unfortunately, predicting waste layer SWCCs as waste undergoes physical and biological changes is difficult and there is a lack of data in relevant literature. Once

preferential flow is introduced, the waste layer parameters have very little influence and all simulations produced approximately the same amount of percolation (Figure 4-11b).

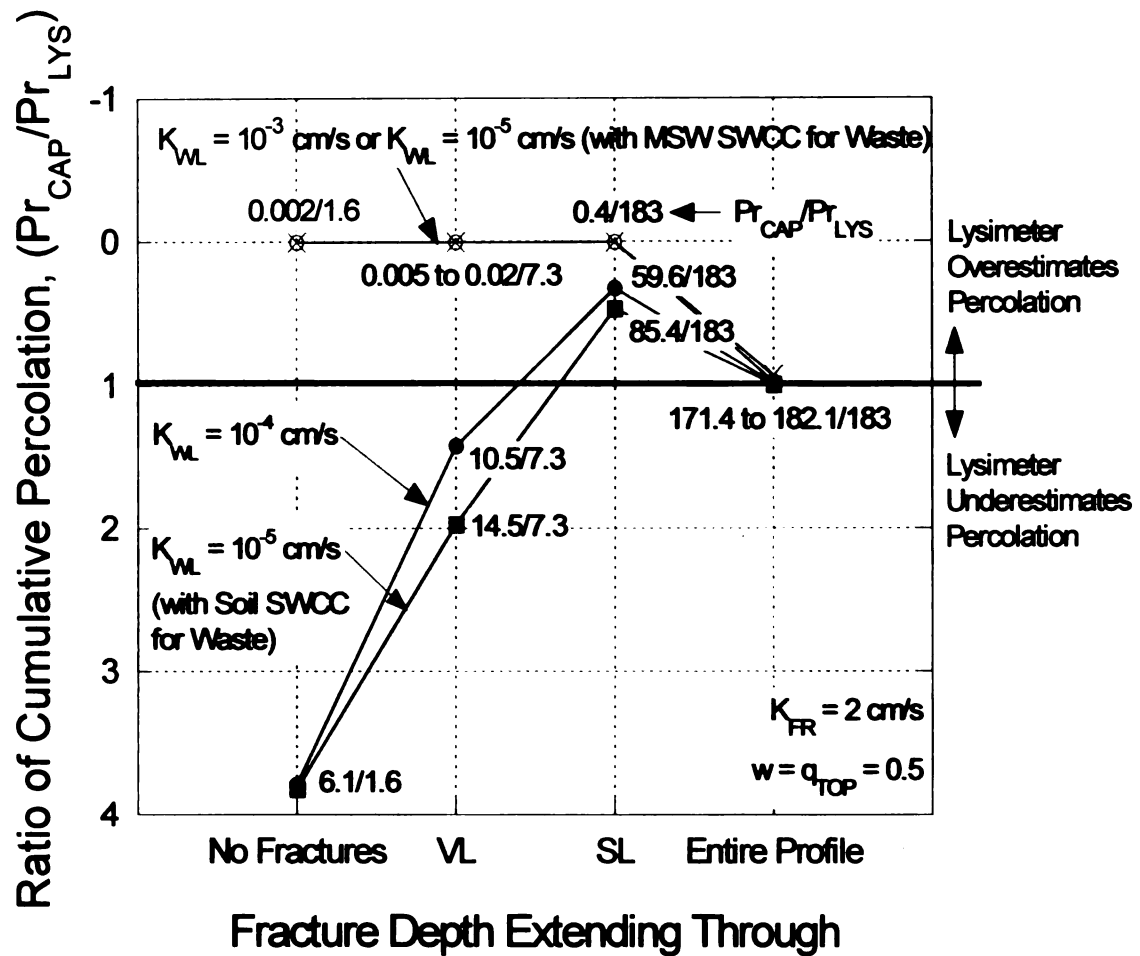


Figure 4-12: Ratio of Cumulative Percolation with Varying Fracture Depths and Waste Layer Hydraulic Conductivity.

Figure 4-12 shows the ratio of cumulative percolation through the cap to that for the lysimeter for varying depths of the fracture network and varying waste layer hydraulic conductivities and SWCCs. This graph is intended to demonstrate that lysimeters may over predict or under predict percolation depending upon the extent of cracks and the unsaturated hydraulic properties of various components. In Figure 4-12, when the ratio is greater than 1, that means the lysimeter over estimated percolation. Figure 4-12 shows that the lysimeter over estimates percolation except when the waste layer hydraulic conductivity is  $10^{-4}$  cm/s and  $10^{-5}$  cm/s when the SWCCs of soils were adapted as input of SWCC for the waste. When the simulation with waste layer hydraulic conductivity of  $10^{-5}$  cm/s was repeated with an MSW SWCC as opposed to a soil SWCC, the lysimeter over estimated percolation. Figure 4-12 demonstrates that lysimeters typically over estimate percolation and also shows the influence the waste SWCC can have on simulated percolation. Clearly, measurement of representative SWCCs and waste hydraulic conductivities is critical if we want to predict the percolation from an actual cap based on the percolation measured from a lysimeter.

#### **4.4.2 Thickness of Waste Layer**

Six simulations were performed to evaluate the effect of waste layer thickness on percolation. Waste layer thicknesses equal to 3.05 m, 6.1 m and 12.2 m were simulated. All simulations had a hydraulic conductivity of  $10^{-3}$  cm/s,  $10^{-5}$  cm/s, and  $10^{-3}$  cm/s for the vegetation, storage, and waste layer, respectively. When preferential flow was simulated, fractures extended through the waste layer with a hydraulic conductivity of 2 cm/s. Vertical discretization of mesh nodes was 300, 750 and 900 for the 3.05 m, 6.1 m, and 12.2 m waste layer respectively. The water balance error for the simulations was

approximately 30%. As seen in Figure 4-13 waste layer thickness does not influence percolation amounts into the waste layer for the thicknesses simulated in this study.

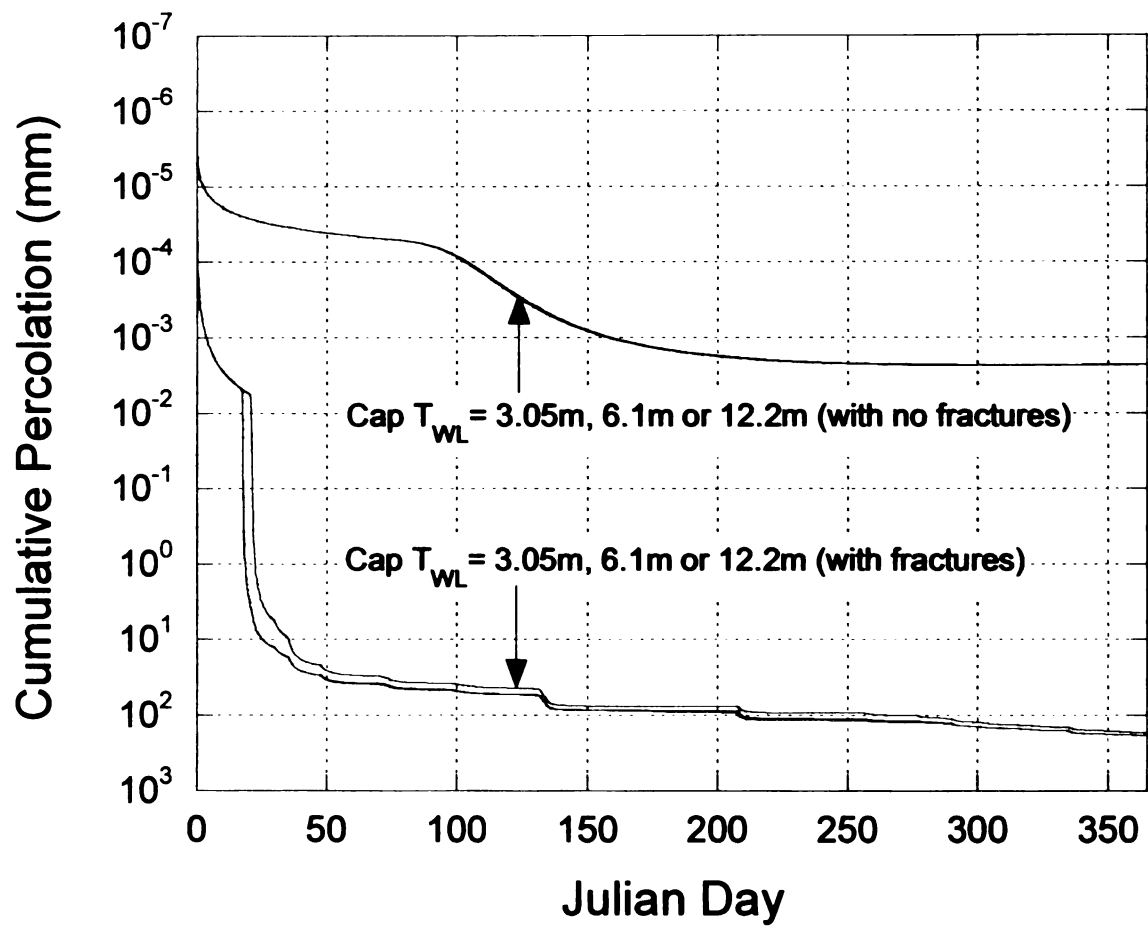


Figure 4-13: Effect of Waste Layer Thickness on Simulated Percolation.

## **CHAPTER 5**

### **SUMMARY AND CONCLUSIONS**

In this study, parameters impacting percolation into the waste layer of an evapotranspirative landfill cover with preferential flow was evaluated using HYDRUS-2D (beta v1.04) and HYDRUS-1D (v4.05). Simulations consisted of either a two layer soil cover without an underlying waste layer (lysimeter) or the same cover with a waste layer (cap). The purpose of these simulations was to evaluate: (1) percolation measured using lysimeters does not equate to the percolation across the cap and waste boundary because lysimeters exclude the presence of a waste layer and evapotranspirative gradients at the interface; and (2) when only capillary flow is considered and flow through fractures is ignored percolation is under-estimated.

Simulation duration, the presence of preferential flow, preferential flow pathway depth, hydraulic conductivity of fractures, the volume of fractures, surface flow entering the fractures, hydraulic conductivity of the storage layer, hydraulic conductivity and soil-water retention properties of the waste layer, and waste layer thickness were varied throughout multiple simulations. The cumulative percolation of water across the storage layer-waste layer boundary (bottom of cap) was used to assess the performance of the cap versus a lysimeter. Based on the results of the simulations, the following conclusions were drawn:

1. When preferential flow is absent, lysimeters over-predict percolation compared to a cap. When preferential flow is present, lysimeters either over-

predict percolation or the percolation is about the same depending upon the fracture depth and hydrologic properties of the storage and waste layer.

2. When preferential flow is considered, percolation in both the lysimeter and cap increases.
3. Waste layer thickness does not affect percolation when it is greater than the thickness of the cap.
4. Fracture hydraulic conductivity has minimal influence on percolation when it is  $> 0.2$  cm/s.
5. As the depth of preferential flow paths is increased, the magnitude of percolation increases.
6. The relative volume of the fracture domain had little influence on percolation when the fraction of precipitation entering the fracture network is not proportionately changed.
7. The hydraulic conductivity of the storage layer influences percolation only when preferential flow is not present. As the storage layer hydraulic conductivity increases, so does the percolation. When preferential flow in the storage layer is considered, the preferential flow dominates and the hydraulic conductivity of the matrix does not influence percolation.
8. The hydraulic conductivity of the waste layer influences percolation when only capillary flow is considered. As the waste layer hydraulic conductivity increases, percolation decreases. When preferential flow is considered, it dominates water flow and the hydraulic conductivity of the waste does not influence percolation.

9. The SWCC and hydraulic conductivities of the waste greatly influences percolation and hence the relative percolation between a cap and an equivalent lysimeter.

The key conclusion of this study is that preferential flow can significantly increase percolation through the cap into the waste layer of a landfill. Ignoring preferential flow, whether it is currently present or will be in the future, can be detrimental when designing and evaluating landfill final covers. HYDRUS was able to simulate percolation trends through an ET cover but with some numerical challenges. The dual-permeability model was often unstable. Simulations often crashed and the number of vertical mesh nodes had to be decreased making the mesh coarse which produces less accuracy in the results. Simulations that would run in HYDRUS-2D would not run in HYDRUS-1D unless the water and pressure tolerances were changed. In HYDRUS-1D,  $q_{TOP}$  was a parameter that could be changed in the input menu but all simulations crashed when  $q_{TOP}$  was anything but 0.5.  $q_{TOP}$  is “hard-coded” in HYDRUS-2D as 0.5 and hence could only be changed from the “back-end” of the input.

With a program that crashes frequently at what appears to be a random manner, it is difficult to have confidence in the results. When a simulation does crash, there is no indication as to why and the user must blindly change the tolerances, iteration number, and number of mesh nodes in an attempt to make the simulation run. In order for dual-permeability models to become a reliable method of predicting percolation through a landfill cover, numerically stable models need to be developed.

## REFERENCES

- Albright, W.H., Benson, C.H., Gee, G.W., Roesler, A.C., Abichou, T., Apiwantragoon, P., Lyles, B.F., and Rock, S.A. (2004). "Field water balance of landfill final covers." *J. Environ. Qual.*, 33, 2317-2332.
- Benson, C.H., and Wang, X. (1998) "Soil water characteristic curves for solid waste." Environmental Geotechnics Report 98-13, Dept. of Civil and Env. Eng., U of Wisconsin-Madison.
- Benson, C.H., Bohnhoff, G.L., Ogorzalek, A.S., Shackelford, C.D., Apiwantragoon, P., and Albright, W.H. (2005) "Field data and model predictions for a monolithic alternative cover." *Waste Containment and Remediation*, ASCE Geotechnical Special Publication No. 47.
- Cameira, M.R., Ahuja, L., Fernando, R.M. and Pereira, L.S. (2000). "Evaluating field measured soil hydraulic properties in water transport simulations using the RZWQM." *J. of Hydrology*, 236, 78-90.
- Daniel B. Stephens & Associates, Inc. (2006) "Laboratory report for Waste Management, Inc. (Woodland Meadows samples)." Daniel B. Stephens & Associates, Inc., Albuquerque, New Mexico.
- Gärdenäs, A., Šimůnek, J., Jarvis, N., and van Genuchten, M.Th. (2006) "Two-dimensional modeling of preferential water flow and pesticide transport from a tile-drained field." *J. of Hydrology*, 329, 647-660.
- Gerke, H.H., Köhne, J.M. (2004) "Dual-permeability modeling of preferential bromide leaching from a tile-drained glacial till agricultural field." *J. of Hydrology*, 289, 239-257.
- Hauser, V.L., P.E., Weand, B.L. and Gill, M.D., P.E. (2001). "Natural covers for landfills and buried waste." *J. of Env. Eng.*, Vol. 127, No. 9, 768-775.
- Jacobson, J.J., Heydt, H., Piet, S., Sehlke, G., Soto, R., and Visser, J. (2005). "Dynamic modeling of an evapotranspiration cover." *Practice Periodical of Hazardous, Toxic, and Radioactive Waste management*, Vol. 9, No. 4, 223-236.
- Jarvis, N.J. (1998) "Modeling the impact of preferential flow on nonpoint source pollution." In: Selim, H.M., Ma, L. (Eds.), *Physical Nonequilibrium in Soils: Modeling and Application*, 195-221.
- Khire, M.V., Benson, C.H., and Bosscher, P.J. (1997). "Water balance modeling of earthen final covers." *J. of GeoTech. and GeoEnv. Eng.*, Vol. 123, No. 8, 744-754.

- Khire, M.V., Benson, C.H., and Bosscher, P.J. (1999). "Field data from a capillary barrier and model predictions with UNSAT-H." *J. of GeoTech. and GeoEnv. Eng.*, Vol. 125, No. 6, 518-527.
- Khire, M.V., Benson, C.H., and Bosscher, P.J. (2000). "Capillary barriers: design variables and water balance." *J. of GeoTech. and GeoEnv. Eng.*, Vol. 126, No. 8, 695-708.
- Khire, M.V. and Mijares, R.G. (2008). "Influence of the waste layer on percolation estimates for earthen caps located in a sub-humid climate." *Waste Management and Remediation*, ASCE GeoCongress 2008, New Orleans.
- Kodešová, R., Kozák, J., Šimůnek, J., and Vacek, O. (2005) "Single and dual-permeability models of chlorotoluron transport in the soil profile." *Plant and Soil Env.*, 51, 7, 310-315.
- Morris, C.E., and Stormont, J.C., Members, ASCE (1997). "Capillary barriers and subtitle D covers: estimating equivalency." *J. of Env. Eng.*, Vol. 123, No. 1, 3-10.
- Novák, V., Šimůnek, J., and van Genuchten, M. Th. (2000). "Infiltration of water into soil with cracks." *J. or Irrigation and Drainage Eng.*, Vol. 126, No. 1, 41-47.
- Ogorzalek, A.S., Bohnhoff, G.L., Shackelford, C.D., Benson, C.H., and Apiwantragoon, P. (2008) "Comparison of field data and water-balance predictions for a capillary barrier cover." *J. of GeoTech. and GeoEnv. Eng.*, Vol. 134, No. 4, 470-486.
- Sadek, S., Ghanimeh, S., and El-Fadel, M. (2007) "Predicted performance of clay-barrier landfill covers in arid and semi-arid environments." *Waste Management*, 27, 572-583.
- Scanlon, B.R., Reedy, R.C., Keese, K.E and Dwyer, S.F. (2005). "Evaluation of evapotranspirative covers for waste containment in arid and semiarid regions in the southwestern USA." *Vadose Zone Journal*, 4, 55-71.
- Šimůnek, J., Šejna, M., and van Genuchten, M.Th. (1999) "The HYDRUS-2D software package for simulating two-dimensional movement of water, heat, and multiple solutes in variably saturated media." Version 2.0, IGWMC-TPS-53, International Ground Water Modeling Center, Colorado School of Mines, Golden, Colorado.
- Šimůnek, J., Jarvis, N.J., van Genuchten, M.Th. and Gärdenäs, A. (2003) "Review and comparison of models for describing non-equilibrium and preferential flow and transport in the vadose zone." *J. of Hydrology*, 272, 14-35.
- Simunek, J., Sejna, M., Saito, H., Sakai, M., and van Genuchten, M.Th. (2008a) "The HYDRUS-1D software package for simulating the one-dimensional movement of water, heat, and multiple solutes in variably-saturated media." Version 4.0,

Department of Environmental Sciences, University of California Riverside, Riverside, California.

Simunek, J., van Genuchten, M.Th., and Sejna, M. (2008) "Development and applications of the HYDRUS and STANMOD software packages and related codes." *Vadose Zone J.*, Vol 7, 587-600.

U.S. DOE (U. S. Department of Energy), Office of Environmental Management and the Office of Science and Technology (2000). "Alternative Landfill Cover." Innovative Technology Summary Report.

USEPA (U.S. Environmental Protection Agency) (1997) Resource Conservation and Recovery Act Information System (RCRAIS) database, EPA National Oversight Database.

Vogel, T., Gerke, H.H, Zhang, R., and van Genuchten, M.Th. (2000) "Modeling flow and transport in a two-dimensional dual-permeability system with spatially variable hydraulic properties." *J. of Hydrology*, 238, 78-89.

MICHIGAN STATE UNIVERSITY LIBRARIES



3 1293 03062 5119